Baryons in a relativized quark model with chromodynamics

Simon Capstick* and Nathan Isgur
Department of Physics, University of Toronto, Toronto, Canada M5S 1A7
(Received 24 January 1986)

We have studied the three-quark system in a relativized version of the quark potential model with chromodynamics. With parameters consistent with those of an analogous study of the $q\bar{q}$ system, we obtain a good description of the known baryons. Our model generally supports the *phenomenology* of nonrelativistic calculations: it naturally explains the apparent absence of spin-orbit interactions in baryons, and leads to spectra and internal compositions for the baryons which are qualitatively similar to those of the usual nonrelativistic model.

I. INTRODUCTION

The baryons have historically played a central role in the development of the theory of the strong interaction. The low-lying baryons were crucial to the motivation for the fractionally charged quark model[1] and soon after its proposal baryon spectroscopy,[2] static properties, and decays[3,4] played a major role in the development of the quark model as a dynamical theory. Later, the attempt to place this dynamics on a sounder footing led to the idea of color[5] and eventually to quantum chromodynamics[6] (QCD).

More recently, the quark model with chromodynamics has provided some of the more convincing qualitative tests of QCD in the nonperturbative regime. While the most rigorous of these tests have been in heavy quarkonia, it can be argued that the most impressive facet of the "QCD-improved quark model"[7,8] has been its ability to explain, at least schematically, the vast body of information available on light-quark mesons[9] and baryons.[10,11]

The most widely applied model of this type has been the quark potential model.[7,8] Its success can only claim to be qualitative, despite its surprising ability to make quantitative predictions, because in its usual form it is not very well founded. Among the most prominent flaws of the usual treatment are the following.

(1) Nonrelativistic quark motion. Both the light constituent-quark masses and their momenta must be of order $\Lambda_{\rm QCD} \sim b^{1/2}$ (where $\Lambda_{\rm QCD}$ is the QCD scale parameter and b the string tension), so that p/m will necessarily be of order unity. Thus, a nonrelativistic treatment of such motion will clearly be inaccurate. (Note, however, that the motion is not ultrarelativistic; this is presumably why the nonrelativistic approximation is nevertheless useful.) That $p/m \sim 1$ is, of course, also found by explicit calculations.

(2) Nonrelativistic quark dynamics. A corollary of (1) is that a nonrelativistic expansion of the interquark potential will also be inaccurate (though once again it may be qualitatively useful). In particular, the usual Breit-Fermi-type interactions may be expected to be inaccurate in two ways: (a) Mass factors, for example those like $1/m_i m_j$ characteristic of the important color-magnetic interactions, can become momentum dependent—indeed, for relativistic on-shell scattering, one often finds such factors replaced by the quark energies; (b) the radial dependencies of the $p/m \to 0$ limit can be modified by the characteristic smearing of a relativistic quark coordinate as well as by nonleading momentum-transfer dependence in the potentials.

(3) The neglect of gluon dynamics. The quark potential model's wave functions refer only to the quark coordinates, but in QCD the wave function of a hadronic system must also specify the state of the glue.

(4) The neglect of scale dependence. In an interacting field theory, the state vector of a system will always depend on the ultraviolet cutoff (a mass M or a lattice spacing a) of the theory. Thus, the quark-model wave function of the system should explicitly refer to this cutoff scale. This scale dependence is analogous to the scale dependence of deep-inelastic structure functions, and related to the distinction between current and constituent quarks.

Given these serious flaws, it might be considered surprising that the usual quark potential model works as well as it does. However, the reasons for this success can perhaps be understood: the defects just described can, we believe, often be hidden in the choice of such effective parameters as the constituent-quark mass (which can partially absorb extra quark kinetic energy), the string tension (which can partially absorb deviations in the quark kinetic energy with excitation as well as some of the effects of the hidden gluonic degrees of freedom), and α_s (which can absorb some of the effects of relativistic modifications of spin-dependent interactions). Thus the flaws of the usual model would only become apparent if the *fundamental* values of these parameters were used in the model Hamiltonians.

We believe that the baryon "spin-orbit puzzle"—the mysterious absence of spin-orbit forces of the strength expected in the nonrelativistic limit[10,12] is simply an example of a case where it has proved to be impossible to hide the flaws of the nonrelativistic models. We will see in the following, on the other hand, that this puzzle is naturally explained once the flaws of the usual treatment are corrected.

II. THE QUARK MODEL REEXAMINED

Two recent developments allow us to at least begin to place the quark potential model on a firmer foundation. The first of these developments emerges from a better understanding of the status of the quark model within QCD; the second comes from considering the effects $p/m \sim 1$ will have in modifying the nonrelativistic quark model.

The flux-tube model for QCD (Ref. 13) naturally suggests an interpretation of the quark model within QCD. This interpretation not only clarifies the status of the quark model, but also helps to rationalize its ability to describe the low-lying hadrons without explicit reference to the gluonic degrees of freedom. The flux-tube model is based on a resummation of the strong-coupling lattice Hamiltonian for QCD which leads to an interpretation of the properties of the theory in terms of quarks and flux tubes (which are stringlike). At short distances (i.e., small coupling) the flux-tube basis is not very economical, but at large distances it suggests a simple picture of the strong interactions in terms of weakly perturbed quantum strings.

To appreciate the status of the quark model in this picture, consider first a set of static quark sources at the points $\mathbf{r}_1,\mathbf{r}_2,\ldots,\mathbf{r}_N$. In the presence of these sources the glue will have a set of eigenenergies $E_i(\mathbf{r}_1,\mathbf{r}_2,\ldots,\mathbf{r}_N)$ with $i=1,2,\ldots$. Each of these $3N$-dimensional gluonic energy surfaces thus corresponds to an adiabatic quark potential, and we can define the quark-model limit as corresponding to the case where the system can be well approximated by quark motion on the *lowest adiabatic surface.* Since, in the absence of pair creation, confinement ensures that there will be a mass gap between E_0 and E_1 in the $q\bar{q}$ and qqq systems (but not in general elsewhere), it is clear that this limit will exist for at least the low-lying states of heavy-quark mesons and baryons where $\omega_{\text{quark}} \ll \omega_{\text{gap}}$. Whether or not this approximation is ever valid for light-quark systems will depend on detailed properties of the adiabatic surfaces, but within the flux-tube model for these surfaces, it has been possible to show[14] that it is *very* accurate for $b\bar{b}$ and $c\bar{c}$ and accurate enough in the light-quark sectors to be corrected perturbatively. The flux-tube model thus allows us to understand the ability of the quark model to avoid a specification of the state of the glue: quark-model wave functions had a "suppressed subscript" indicating that the glue was (approximately) in its (adiabatically evolving) ground state. Of course, quark motion in the excited adiabatic surfaces should also exist: such states correspond to as yet undiscovered hybrid mesons and baryons.

The flux-tube model also allows us to understand the scale dependence of hadronic state vectors. At small lattice spacings (or large ultraviolet cutoff masses M) the hadronic state will be very complex: in this limit the quarks are current quarks (so that light current quark pairs will be plentiful), elaborate flux-tube topologies [containing, for example, branching flux-tube lines with elements in nonfundamental representations of SU(3)] are not suppressed, and the vacuum is full of disconnected fluctuations of localized flux and of localized $q\bar{q}$ pairs. Thus, while we are allowed to choose any scale we like to describe a hadron, this description will be simplest if we choose the *largest* spatial scale that is fine enough to accurately describe the hadron. For a light-quark system with a typical diameter of the order of 2 fm, this cutoff scale will be of the order of 0.2 fm; such a coarse-grained (constituent) quark will obviously have an effective mass which includes the nearby gluonic energy, i.e., $m \sim ba \sim \Lambda_{\text{QCD}} \sim 200$ MeV. A heavy-quark system will have a size typified by $(m_Q\alpha_s)^{-1}$ and so will require a cutoff of order $m_Q{}^{-1}$. Its effective mass will thus approach its current-quark mass as $m_Q \to \infty$. (It is this limit that corresponds to the usual atomic physics case where scale dependence is only a weak logarithmic effect.)

The second development which allows us to proceed to a more solid foundation for the quark model results from some recent studies of the relativization of the quark model. These studies are based on the observation that with $p/m \lesssim 1$, relativistic effects should be parametrizable as smooth departures from the established nonrelativistic limit appropriate to heavy quark systems. In Ref. 15 it was shown that typical light quark momentum wave functions, when convoluted with exact free (relativistic) spinor matrix elements, could preserve all of the good predictions of the quark model for dynamical matrix elements (like those responsible for baryon magnetic moments or meson magnetic dipole decays) while improving such bad predictions as G_A/G_V and the matrix element $\langle 0 | A^\mu | A_1 \rangle$ where A_1 is the ${}^3P_1$ $I=1$ meson. The preservation of the good results of the nonrelativistic limit in this scheme only required the assignment of a new smaller value for the (otherwise unconstrained) constituent-quark mass, in accord with the comments made earlier.

On the basis of these encouraging results, Ref. 16 implemented a full "relativization" of the quark model for mesons. This program, which is the analogue of the program described in this paper, demonstrated that with an adjusted set of basic parameters (like the quark masses) appropriate to the relativized quark model, and a certain number of nonfundamental parameters (used to describe qualitatively the expected relativistic modifications of the interquark interactions described in the Introduction), it is possible to produce a unified treatment of all mesons from the lightest to the heaviest known, in which the quark model defects discussed above are at least partially remedied. Since the "relativistic parameters" of this program were not derived from first principles, the results of Ref. 16 can only be considered as a demonstration that (1) the desirable characteristics of the quark potential model can survive relativization, and (2) when relativized, the description of mesons can be unified in terms of a well-founded model with a single set of parameters. Of course, it remains to be shown that the relativistic modifications which appear in that model follow from the underlying (cutoff) field theory.

It also remains to demonstrate that the same program will succeed in describing baryon spectroscopy, thereby unifying mesons and baryons as it unifies the different meson families. The demonstration of this remarkable fact is the main subject of this paper.

III. THREE QUARKS IN A RELATIVIZED QUARK MODEL WITH CHROMODYNAMICS

Our model for the three-quark system is the immediate and essentially unique generalization of the model of Ref. 16 from $q\bar{q}$ to qqq. We nevertheless briefly describe it again here for completeness. Our program is to solve the rest-frame equation

$$H\,|\Psi\rangle = E\,|\Psi\rangle \tag{1}$$

in the qqq sector of Fock space where

$$H = H_0 + V \tag{2}$$

in which

$$H_0 = \sum_{i=1}^{3} (p_i^2 + m_i^2)^{1/2} \tag{3}$$

and V is a relativized three-quark momentum-dependent potential. The momentum dependence of V will arise both from on-shell relativistic modifications and from integrating out higher components of Fock space. In the *nonrelativistic limit*

$$V \underset{p/m\to 0}{\longrightarrow} V_{\rm conf} + V_{\rm oge}\ , \tag{4}$$

where $V_{\rm conf}$ consists of the three-body adiabatic potential $V_{\rm string}$ generated by the quantum ground state of the Y string configuration (see Fig. 1) and a spin-orbit term arising from the adiabatic potential via Thomas precession, and where $V_{\rm oge}$ is the usual Breit-Fermi interaction including a Coulomb term, hyperfine interactions, and the spin-orbit interactions. More explicitly, in this limit

$$V \to V_{\rm si} + V_{\rm sd}\ , \tag{5}$$

where the spin-independent interaction is

$$V_{\rm si} = V_{\rm string} + V_{\rm Coul}\ , \tag{6}$$

where

$$V_{\rm Coul} \to \sum_{i<j} V_{ij}^{\rm Coul} = \sum_{i<j} -\frac{2\alpha_s(r_{ij})}{3r_{ij}} \tag{7}$$

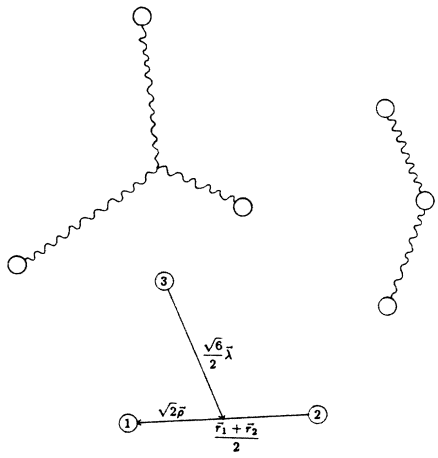

FIG. 1. The gauge-invariant string configurations and the relative coordinates ρ and λ.

and where the spin-dependent interaction is

$$V_{\rm sd} = V_{\rm hyp} + V_{\rm so} \tag{8}$$

with the hyperfine interaction

$$V_{\rm hyp} \to \sum_{i<j} \frac{2\alpha_s}{3m_i m_j}\left[\frac{8\pi}{3}\mathbf{S}_i\cdot\mathbf{S}_j\delta^3(\mathbf{r}_{ij}) + \frac{1}{r_{ij}^{\,3}}\left[\frac{3\mathbf{S}_i\cdot\mathbf{r}_{ij}\mathbf{S}_j\cdot\mathbf{r}_{ij}}{r_{ij}^{\,2}} - \mathbf{S}_i\cdot\mathbf{S}_j\right]\right], \tag{9}$$

consisting of the Fermi contact term $\propto\delta^3(\mathbf{r}_{ij})$ and a tensor term, and the spin-orbit interaction

$$V_{\rm so} = V_{\rm so(cm)} + V_{\rm so(TP)} \tag{10}$$

with a color-magnetic piece

$$V_{\rm so(cm)} \to \sum_{i<j} \frac{2\alpha_s}{3r_{ij}^{\,3}}\left[\frac{\mathbf{r}_{ij}\times\mathbf{p}_i\cdot\mathbf{S}_i}{m_i^2} - \frac{\mathbf{r}_{ij}\times\mathbf{p}_j\cdot\mathbf{S}_j}{m_j^2} - \left[\frac{\mathbf{r}_{ij}\times\mathbf{p}_j\cdot\mathbf{S}_i - \mathbf{r}_{ij}\times\mathbf{p}_i\cdot\mathbf{S}_j}{m_i m_j}\right]\right] \tag{11}$$

and a Thomas-precession piece

$$V_{\rm so(TP)} \to -\sum_{i<j} \frac{1}{2r_{ij}}\frac{\partial V_{\rm si}}{\partial r_{ij}}\left[\frac{\mathbf{r}_{ij}\times\mathbf{p}_i\cdot\mathbf{S}_i}{m_i^2} - \frac{\mathbf{r}_{ij}\times\mathbf{p}_j\cdot\mathbf{S}_j}{m_j^2}\right] \tag{12}$$

which includes the effects of the full spin-independent potential. In these formulas m_i, $\mathbf{p}_i$, and $\mathbf{S}_i$ are the mass, momentum, and spin of the ith quark in the baryon center-of-momentum frame, and the quantities $\mathbf{r}_{ij} = \mathbf{r}_i - \mathbf{r}_j$ are the relative positions of the (ij) pair of quarks. Note that we have shown explicitly here only the leading term of each tensor type which appears in an expansion in p/m; the reason for this will appear momentarily.

Of course, as already stressed, *this $p/m \to 0$ limit is not applicable to systems containing a light quark;* it is given here mainly for orientation, while the actual momentum-dependent potentials used in our calculations are discussed below. In Appendix A we list these potentials; here we will illustrate the modifications we make to this limit by explicit reference to the contact term of the hyperfine interaction. As already mentioned, there are two kinds of

relativistic effects to be considered: (1) the strength of the interactions can depend on the energy of the interacting quarks [the interaction of a quark can depend on $\mathbf{P}=\frac{1}{2}(\mathbf{p}+\mathbf{p}')$ where $\mathbf{p}$ and $\mathbf{p}'$ are its initial and final momenta] and (2) the spatial shape of the interaction potentials can change [the interaction can depend on $\mathbf{Q}=\mathbf{p}-\mathbf{p}'$ in ways that modify the Fourier transforms in $\mathbf{Q}$ represented by the $\mathbf{r}$ dependences of Eqs. (5)–(12); these shapes will also be modified by the required ultraviolet cutoff of the theory]. We parametrize these two kinds of effects in terms of two mechanisms by taking, for example,

$$V_{ij}^{\text{cont}}=\left[\frac{m_i m_j}{E_i E_j}\right]^{1/2+\epsilon_{\text{hyp}}}\left[\frac{2\mathbf{S}_i\cdot\mathbf{S}_j}{3m_j m_j}\nabla^2\tilde{V}_{ij}^{\text{Coul}}\right]\times\left[\frac{m_i m_j}{E_i E_j}\right]^{1/2+\epsilon_{\text{hyp}}}, \tag{13}$$

where $\tilde{V}_{ij}^{\text{Coul}}$ is V_{ij}^{Coul} of Eq. (7) smeared over a distribution

$$\rho_{ij}(\mathbf{r}-\mathbf{r}')=\frac{\sigma_{ij}{}^3}{\pi^{3/2}}e^{-\sigma_{ij}{}^2(\mathbf{r}-\mathbf{r}')^2} \tag{14}$$

of the interquark coordinate. We relegate the details of this procedure to Appendix A, but it is clear that the (m/E) factors, the importance of which is governed by ϵ_{hyp}, will modify both the $\mathbf{P}$ and $\mathbf{Q}$ dependence of the interaction, while the smearing with ρ_{ij} will modify its shape in $\mathbf{r}_{ij}$ directly. Clearly this method of relativizing the quark model is very crude, but since $p/m\simeq 1$ is not too far from the nonrelativistic regime, we can expect it to correctly parametrize the main characteristics of these relativistic effects.

To complete the definition of the model, we describe our treatment of α_s. With N_f quark flavors with masses much less than Q^2, in lowest-order QCD

$$\alpha_s(Q^2)=\frac{12\pi}{(33-2N_f)\ln(Q^2/\Lambda_{\text{QCD}}{}^2)}. \tag{15}$$

Since $\Lambda_{\text{QCD}}\simeq 200$ MeV, $\alpha_s(Q^2)$ is small for $Q^2\gtrsim 1$ GeV^2, but as $Q\to\Lambda_{\text{QCD}}$, this perturbative formula diverges, signaling the onset of confinement. Since we are working in this soft regime, we cannot avoid this divergence, and so we assume that $\alpha_s(Q^2)$ saturates at some critical value $\alpha_s^{\text{critical}}$ as $Q^2\to 0$. We parametrize this behavior in the convenient form

$$\alpha_s(Q^2)=\sum_{k=1}^{k_{\max}}\alpha_k e^{-Q^2/4\gamma_k{}^2}, \tag{16}$$

where

$$\sum_{k=1}^{k_{\max}}\alpha_k\equiv\alpha_s^{\text{critical}} \tag{17}$$

is a free parameter, but where the remaining parameters are constrained to follow the behavior (15); the resulting fit with $k_{\max}=3$ is shown in Fig. 2. The form (16) is convenient because it is easily transformed into

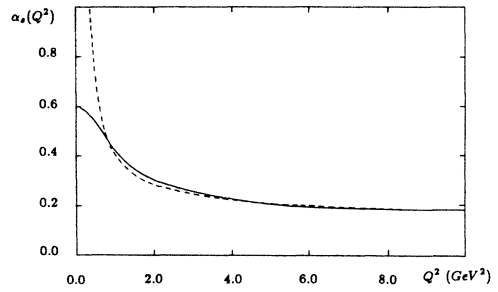

FIG. 2. The leading-order formula (15) for the effective coupling constant with $\Lambda_{\text{QCD}}=200$ MeV and our fit $\alpha_s(Q^2)=0.25e^{-Q^2}+0.15e^{-Q^2/10}+0.20e^{-Q^2/1000}$ (Q^2 in GeV^2).

$$\alpha_s(r)=\sum_k\frac{2\alpha_k}{\sqrt{\pi}}\int_0^{\gamma_k r}e^{-x^2}dx \tag{18}$$

and because it is easily convoluted with the relativistic smearing (14). Once again details can be found in Appendix A.

Not only is our basic model identical to that of the analogous study of $q\bar{q}$ spectroscopy in Ref. 16, but we have also insisted that all of our parameters be close to those determined by that study. The only really new parameter of our model is an overall constant in the three-quark string potential (see Appendix A) relative to the $q\bar{q}$ string potential. This constant is associated with vacuum modifications which are not at the moment calculable. Our parameters are listed in Table I where they are compared to those of meson spectroscopy. The effects of the small modifications we were allowed to make in the

TABLE I. The parameters of the relativized quark potential model. Note that we ignore isospin violation.

	This work	Ref. 16
$\frac{1}{2}(m_u+m_d)$ (MeV)	220	Same
m_s (MeV)	419	Same
m_c (MeV)	1628	Same
m_b (MeV)	4977	Same
b (GeV^2)	0.15	0.18
$\alpha_s^{\text{critical}}$	0.60	Same
Λ_{QCD} (MeV)	200	Same
$C_{q\bar{q}}$ (MeV)	Not applicable	$\frac{4}{3}(-253)=-340$
C_{qqq} (MeV)	−615	Not applicable
σ_0 (GeV)	1.80	Same
s	1.55	Same
$\frac{1}{2}+\epsilon_{\text{cont}}$	$\frac{1}{2}-0.168$	Same
$\frac{1}{2}+\epsilon_{\text{tens}}$	$\frac{1}{2}-0.168$	$\frac{1}{2}+0.025$
$\frac{1}{2}+\epsilon_{\text{so}(v)}$	$\frac{1}{2}$	$\frac{1}{2}+0.055$
$\frac{1}{2}+\epsilon_{\text{so}(s)}$	$\frac{1}{2}+0.30$	$\frac{1}{2}+0.055$
$\frac{1}{2}+\epsilon_{\text{Coul}}$	$\frac{1}{2}$	Same

meson parameters are discussed in more detail in Sec. V below. Suffice it to say that, with *exactly* the meson parameters of Ref. 16, we obtained already a remarkable description of the baryons. As examples, we mention $\Delta-N\simeq 300$ MeV showing that the ρ-π and Δ-N splittings appear to have the same origin, $\Sigma-\Lambda\simeq 80$ MeV showing that the physics of the ratio of K^*-K to ρ-π also appears to operate in the baryons, and $N^*\frac{5}{2}^- - \Delta\simeq 440$ MeV showing that this splitting and the A_2-ρ splitting appear to have the same dynamical origin.

IV. METHODS

While the formulas of Sec. III are a straightforward generalization of those of mesons, the methods one must use to solve for the baryons are naturally more involved. Although most of the details of our methods will be relegated to Appendix B, in this section we outline our procedure.

Even for mesons it is impossible to solve for the eigenfunctions and eigenenergies of the Hamiltonian (with its relativistic kinetic energies, momentum-dependent potentials, tensor and spin-orbit mixings, etc.) directly: one must resort to the use of variational methods. As was done with the mesons,[16] we take as trial wave functions an expansion of the true wave functions in a large harmonic-oscillator basis. [In practice the most convenient method of doing this is to diagonalize the Hamiltonian in a large harmonic-oscillator-based space as a function of a single variational parameter (see below).] This basis has the overwhelming advantage over other choices that its conversion to momentum space—essential for the evaluation of our many momentum-dependent operators—can be done analytically.

One of the main new difficulties with the three-body problem is that it is nontrivial to actually construct all of the allowed states with given quantum numbers out of the available flavor, spin, and orbital wave functions: there are three flavors, three spins, and two relative coordinates, and this much richer structure must now be combined in a way which is consistent with the Pauli principle. To construct the set of possible wave functions for u, d, and s quarks, for example, one would normally construct totally antisymmetric states as products of the antisymmetric color-singlet wave function C_A and totally symmetric wave functions obtained as direct products of S_3 irreducible representations Φ in flavor, χ in spin, and ψ in space. In doing so one is choosing to work in an SU(6) basis, which can be convenient even though SU(6) is broken. At first sight, one would think that at least for the $SU(2)_{\text{flavor}}$ part of SU(6) such symmetrized wave functions would be essential. However, this is not true and for technical reasons which will become apparent we found it very convenient to explicitly carry out only a subset of the antisymmetrizations that would be required by the full S_3 group. The flavor wave functions Φ that we used, which are a generalization of the "*uds* basis" of Ref. 10, are given in Table II (see Ref. 17). Note that these wave functions are all either symmetric or antisymmetric under interchange of quarks one and two. The total spin of the three spin-$\frac{1}{2}$ particles can be either $\frac{1}{2}$ or $\frac{3}{2}$ so that as a complete set of spin wave functions χ we can choose

TABLE II. The baryon flavor wave functions Φ.

State	+2	+1	0	−1
N		uud	ddu	
Δ	uuu	uud	ddu	ddd
Λ			$\frac{1}{\sqrt{2}}(ud-du)s$	
Σ		uus	$\frac{1}{\sqrt{2}}(ud+du)s$	dds
Ξ			ssu	ssd
Ω				sss
Λ_c		$\frac{1}{\sqrt{2}}(ud-du)c$		
Σ_c	uuc	$\frac{1}{\sqrt{2}}(ud+du)c$	ddc	
Λ_b			$\frac{1}{\sqrt{2}}(ud-du)b$	
Σ_b		uub	$\frac{1}{\sqrt{2}}(ud+du)b$	ddb

$$\chi^S_{3/2,3/2}=|\uparrow\uparrow\uparrow\rangle,\ \text{etc.}, \tag{19}$$

$$\chi^{M_\rho}_{1/2,1/2}=\frac{1}{\sqrt{2}}(|\uparrow\downarrow\uparrow\rangle-|\downarrow\uparrow\uparrow\rangle),\ \text{etc.}, \tag{20}$$

$$\chi^{M_\lambda}_{1/2,1/2}=-\frac{1}{\sqrt{6}}(|\uparrow\downarrow\uparrow\rangle+|\downarrow\uparrow\uparrow\rangle-2|\uparrow\uparrow\downarrow\rangle),\ \text{etc.} \tag{21}$$

(We have shown only the top state of a JM multiplet; our other wave functions follow the Condon-Shortley convention.) Notice that these spin wave functions are also either symmetric or antisymmetric under interchange of the first two quarks.

Finally, for our spatial wave functions Ψ we took functions with definite total $\mathbf{L}=\boldsymbol{l}_\rho+\boldsymbol{l}_\lambda$ made from a Clebsch-Gordan sum of harmonic-oscillator wave functions in the two relative coordinates

$$\boldsymbol{\rho}\equiv\frac{1}{\sqrt{2}}(\mathbf{r}_1-\mathbf{r}_2) \tag{22}$$

and

$$\boldsymbol{\lambda}\equiv\frac{1}{\sqrt{6}}(\mathbf{r}_1+\mathbf{r}_2-2\mathbf{r}_3) \tag{23}$$

of the three-body problem (see Fig. 1):

$$\Psi_{LMn_\rho l_\rho n_\lambda l_\lambda}=\alpha^3\sum_m C(l_\rho l_\lambda mM-m;LM)\mathcal{N}_{n_\rho l_\rho}(\alpha\rho)^{l_\rho}e^{-\alpha^2\rho^2/2}L_{n_\rho}^{l_\rho+1/2}(\alpha\rho)Y_{l_\rho m}(\Omega_\rho)$$

$$\times\mathcal{N}_{n_\lambda l_\lambda}(\alpha\lambda)^{l_\lambda}e^{-\alpha^2\lambda^2/2}L_{n_\lambda}^{l_\lambda+1/2}(\alpha\lambda)Y_{l_\lambda M-m}(\Omega_\lambda)\ , \tag{24}$$

where the $L_n^{l+1/2}(x)$ are the associated Laguerre polynomials

$$L_n^{l+1/2}(x)=\sum_{m=0}^{n}(-1)^m\binom{n+l+\frac{1}{2}}{n-m}\frac{x^{2m}}{m!} \tag{25}$$

(half-integral factorials are defined by the Γ function), and the normalization coefficient $\mathcal{N}_{nl}$ is defined by

$$\mathcal{N}_{nl}=\left[\frac{2n!}{\Gamma(n+l+\frac{3}{2})}\right]^{1/2}. \tag{26}$$

We then expanded the wave function in states of the form

$$|\alpha\rangle=C_A\Phi\sum_{M_L}C(LSM_LM-M_L;JM)$$
$$\times\Psi_{LM_Ln_\rho l_\rho n_\lambda l_\lambda}\chi_{SM-M_L}\,. \tag{27}$$

The states (27) are taken to be explicitly antisymmetric only under interchange of quarks one and two; they are the generalization of the *uds* basis of Ref. 10. In a given sector, we expanded in a restricted set of such states. For example, the proton, with flavor wave function *uud* and $J^P=\frac{1}{2}^+$, must have a spin-space wave function which is symmetric under exchange of quarks 1 and 2. Moreover, the sum over the $|\alpha\rangle$ is restricted to wave functions which have $J=\frac{1}{2}$ and $l_\rho+l_\lambda$ even for positive parity.

The penalty for avoiding the use of the S_3 symmetry group will now be apparent. The most general state consistent with the Pauli principle for the two identical quarks in *uud*, is *too* general: *uud* can also be a Δ^+. While this sounds like an intolerable situation, in practice the penalty is slight. Isospin symmetry guarantees that the eigenstates of the Hamiltonian will be isospin eigenstates (barring accidental degeneracies) so that diagonalization of the Hamiltonian in a (large) set of Pauli-allowed *uud* states automatically leads to a separation of the eigenstates into two noncommunicating blocks of $I=\frac{1}{2}$ and $\frac{3}{2}$ states. For any who might doubt that the slight inconvenience of identifying these blocks and the modest increase in computer time required to carry out the diagonalization are worth tolerating, we suggest the exercise of trying to construct the *uud* states with $I=\frac{1}{2}$ using the available harmonic-oscillator states up to $8\hbar\omega$.

Our program is therefore to calculate the energy eigenstates of the Hamiltonian (2) in the basis of harmonic-oscillator wave functions (27), subject to the restrictions noted above. This is accomplished by forming a matrix of the Hamiltonian operator and diagonalizing this matrix. The harmonic-oscillator wave functions have only the parameter α [see Eq. (24)], and in principle if we expand in an infinitely large basis set, our results would be independent of this parameter. With a truncated set, there exists an α for which the ground-state energy is minimized, one for which the first-excited-state energy is minimized, etc. The Hylleraas-Undheim theorem[18] states that each minimum is separately an upper bound for each energy eigenvalue, i.e., that we may minimize each eigenvalue independently as a function of α. (Of course, if we wish to have a set of approximate wave functions we will have to settle for a single value of α, but we can do better than this for spectroscopy.)

Our problem is now reduced to one of calculating the matrix elements

$$H_{\alpha\beta}=\langle\alpha|H|\beta\rangle\,. \tag{28}$$

There are two important details which we have to explore before explaining the calculation of the various terms in H. The first is that most of the terms in the Hamiltonian are of the form $\sum_{i<j}H_{ij}(r_{ij})$, and so we have to integrate functions of r_{12}, r_{13}, and r_{23}, where

$$r_{12}=\sqrt{2}\rho\,, \tag{29}$$

$$r_{13}=\frac{1}{\sqrt{2}}(\rho^2+\sqrt{3}\mathbf{p}\cdot\boldsymbol{\lambda}+3\lambda^2)^{1/2}\,, \tag{30}$$

$$r_{23}=\frac{1}{\sqrt{2}}(\rho^2-\sqrt{3}\boldsymbol{\rho}\cdot\boldsymbol{\lambda}+3\lambda^2)^{1/2}\,. \tag{31}$$

Since the wave function (27) is *always* antisymmetric under exchange of quarks 1 and 2, we know that

$$\langle\alpha|H_{13}|\beta\rangle=\langle\alpha|H_{23}|\beta\rangle\,, \tag{32}$$

so that

$$\left\langle\alpha\left|\sum_{i<j}H_{ij}(r_{ij})\right|\beta\right\rangle=\langle\alpha|(H_{12}+2H_{13})|\beta\rangle\,. \tag{33}$$

Calculation of the $H_{12}(r_{12})$ matrix elements is straightforward since $\mathbf{r}_{12}=\sqrt{2}\boldsymbol{\rho}$. To perform the r_{13} integration we make a change of variables to

$$\boldsymbol{\rho}'=\frac{1}{\sqrt{2}}(\mathbf{r}_1-\mathbf{r}_3)\,, \tag{34}$$

$$\boldsymbol{\lambda}'=\frac{1}{\sqrt{6}}(\mathbf{r}_1+\mathbf{r}_3-2\mathbf{r}_2)\,, \tag{35}$$

which is the transformation

$$\boldsymbol{\rho}\rightarrow\left[\frac{\boldsymbol{\rho}'}{2}+\frac{\sqrt{3}}{2}\boldsymbol{\lambda}'\right], \tag{36}$$

$$\boldsymbol{\lambda}\rightarrow\left[\frac{\sqrt{3}}{2}\boldsymbol{\rho}'-\frac{\boldsymbol{\lambda}'}{2}\right]. \tag{37}$$

Then in this basis, which we will denote by $|\alpha'\rangle$, the calculation of the H_{13} part of the Hamiltonian becomes identical to that of the H_{12} part in the usual basis. We can therefore specialize our discussion to techniques for calculating matrix elements of the H_{12} terms.

The second problem we have to deal with is the momentum-dependent factors in the Hamiltonian which are combined with spatially dependent potentials. These are dealt with by inserting complete sets (or, rather, practically complete sets: see below) of harmonic-oscillator wave functions between the two types of operators:

$$\left\langle\alpha\left|\left[\frac{m_1m_2}{E_1E_2}\right]^{1/2+\epsilon}V_{12}(r_{12})\left[\frac{m_1m_2}{E_1E_2}\right]^{1/2+\epsilon}\right|\beta\right\rangle=\sum_{\gamma\delta}\left\langle\alpha\left|\left[\frac{m_1m_2}{E_1E_2}\right]^{1/2+\epsilon}\right|\gamma\right\rangle\langle\gamma\,|\,V_{12}(R_{12})\,|\,\delta\rangle\times\left\langle\delta\left|\left[\frac{m_1m_2}{E_1E_2}\right]^{1/2+\epsilon}\right|\beta\right\rangle, \tag{38}$$

and then evaluating the momentum expectation values in the Fourier transform basis, and the potential expectation values in the usual basis. One of the advantages of the harmonic-oscillator basis is that the wave functions are form invariant (up to a phase) under Fourier transformation:

$$\Phi_{nlm}(\alpha;\mathbf{p})=\frac{1}{(2\pi)^{3/2}}\int d^3\mathbf{r}\,e^{-i\mathbf{p}\cdot\mathbf{r}}\Psi_{nlm}(\alpha;\mathbf{r})=(-i)^{2n+l}\Psi_{nlm}\left[\frac{1}{\alpha};\mathbf{p}\right], \tag{39}$$

where

$$\Psi_{nlm}(\alpha;\mathbf{r})=\alpha^{3/2}\mathcal{N}_{nl}(\alpha r)^l Y_{lm}(\Omega)L_n^{l+1/2}(\alpha r)e^{-\alpha^2r^2/2}. \tag{40}$$

Further details of these calculations and the resulting matrix elements are given in Appendix B.

It remains to describe our method of extracting the masses of the various states from the eigenvalues of the Hamiltonian matrix diagonalized in finite wave-function sets. A given wave-function set $\{\,|\,\alpha\rangle\}_{N_{\max}}$ is taken to include all wave functions (subject to the conditions outlined above) up to a given harmonic oscillator $N=2(n_\rho+n_\lambda)+l_\rho+l_\lambda$, which we label $N_{\max}$. $N_{\max}$ is then increased from the minimum required to describe the state of interest, until the energy eigenvalues appear to be approaching a large-$N_{\max}$ limit. Our predictions for the baryon energies are determined by plotting the energy eigenvalue of a state against the inverse of the number of oscillator levels included in its expansion (with the "complete" sets always the largest possible), and then making a linear extrapolation to an infinite number of levels. Let us illustrate this with an example.

The proton, with $J^P=\frac{1}{2}^+$ and with flavor wave function uud, has one harmonic-oscillator wave function at $N=0$, which we may denote $|\,uud\tfrac{1}{2}^+(1)\rangle$, which is of the form [see Eq. (27)]

$$|\,uud\tfrac{1}{2}^+(1)\rangle=C_A\,uud\,\Psi_{000000}\chi^{\lambda}_{1/2,1/2}. \tag{41}$$

Parity rules out all $N=1$ wave functions, and at $N=2$ there are six wave functions which have the correct spin-parity and (12) exchange symmetry. (Two linear combinations of these six have their spin-space wave functions completely symmetric under the permutation group S_3, and so represent Δ's not N's.) The six $N=2$ wave functions are

$$|\,uud\tfrac{1}{2}^+(2)\rangle=C_A\,uud\,\Psi_{001000}\chi^{\lambda}_{1/2,1/2}, \tag{42}$$

$$|\,uud\tfrac{1}{2}^+(3)\rangle=C_A\,uud\,\Psi_{000010}\chi^{\lambda}_{1/2,1/2}, \tag{43}$$

$$|\,uud\tfrac{1}{2}^+(4)\rangle=C_A\,uud\,\Psi_{000101}\chi^{\rho}_{1/2,1/2}, \tag{44}$$

$$|\,uud\tfrac{1}{2}^+(5)\rangle=C_A\,uud\sum_M C(1\tfrac{1}{2}M\tfrac{1}{2}-M;\tfrac{1}{2}\tfrac{1}{2})\times\Psi_{1M0101}\chi^{\rho}_{1/2,1/2-M}, \tag{45}$$

$$|\,uud\tfrac{1}{2}^+(6)\rangle=C_A\,uud\sum_M C(2\tfrac{3}{2}M\tfrac{1}{2}-M;\tfrac{1}{2}\tfrac{1}{2})\times\Psi_{2M0200}\chi^{S}_{3/2,1/2-M}, \tag{46}$$

$$|\,uud\tfrac{1}{2}^+(7)\rangle=C_A\,uud\sum_M C(2\tfrac{3}{2}M\tfrac{1}{2}-M;\tfrac{1}{2}\tfrac{1}{2})\times\Psi_{2M0002}\chi^{S}_{3/2,1/2-M}. \tag{47}$$

Similarly, there are 15 wave functions (either N or Δ) with the correct properties at $N=4$, 28 at $N=6$ and 45 at $N=8$. Or equivalently we need 1, 7, 22, 50, or 95 wave functions to expand the wave function (or the complete sets) up to $N=0$, $N\le2$, $N\le4$, $N\le6$, or $N\le8$. To extract an energy for the first eigenvalue, representing the proton energy, we find the minimum with respect to α of the lowest eigenvalue of the Hamiltonian matrix calculated in the basis with largest $N_{\max}$. We then diagonalize smaller and smaller submatrices of this largest matrix, which correspond to $N\le6$, $N\le4$, $N\le2$, and $N=0$ expansions of the state but always an $N\le8$ expansion of the "complete" sets of wave functions inserted between the space and momentum-space operators. The minimum with respect to α of the lowest eigenvalue of each of these matrices is then plotted against the inverse of the number of oscillator levels included in the expansion of this state, and a linear regression analysis used to extrapolate to infinite $N_{\max}$ and estimate the error in this extrapolated value; the regression includes weights which increase linearly with the number of levels included. In some cases, including that of the proton, the point with only one level (and in this case only one state) in the expansion of the eigenstate is discarded, since removing this point decreases the χ^2 per degree of freedom.

The masses of the excited states of the proton (and the $\Delta\frac{1}{2}^+$ states) are represented by the six next-highest eigenvalues of this Hamiltonian matrix, and of course do not appear until the wave function is expanded up to $N\le2$. Following the process above we may then estimate the $N_{\max}=\infty$ limit of these eigenvalues, with of course a slightly larger error since there will be fewer points in the extrapolation plots for a given $N_{\max}$. In practice the calculations were carried out up to $N\le8$ for the $J^P=\frac{1}{2}^+$ system (for all flavors), and up to $N\le6$ for the other positive-parity states with J^P from $\frac{3}{2}^+$ to $\frac{11}{2}^+$. All negative-parity states (J^P from $\frac{1}{2}^-$ to $\frac{11}{2}^-$) were expanded up to $N\le7$. This meant that for the states with J^P of $\frac{7}{2}^-$, $\frac{9}{2}^\pm$, and $\frac{11}{2}^\pm$ we have only two levels included

in the expansion at $N=N_{\max}$. With these high J states we expect that the convergence should be quite rapid since the wave function is large well away from the origin, and the parts of the Hamiltonian with rapid curvature are all concentrated around the region $\rho=0$ or $\lambda=0$. This turns out to be the case, with the energy eigenvalues dropping only slightly between bases with one and two oscillator levels included. In these cases, rather than put a straight line through these two points (which would be rather artificial), we take the splittings (at $N=6$ or 7) between these states and their nearest like-parity neighbor with three points in its extrapolation, and assume that they remain the same at $N_{\max}=\infty$.

We will discuss the actual errors associated with these methods in Sec. VI below where we discuss our results.

V. RESULTS AND GENERAL COMMENTS

One of the main purposes of this work was to check whether the good results of the usual nonrelativistic model of baryons[10,11] could be both retained and explained in a consistent relativistic framework. We have found that they can be: relativizing the quark model leads naturally (with an appropriate adjustment of such parameters as the quark masses) to a picture of baryon structure that is very similar to the nonrelativistic model of Ref. 10. At the same time, it explains one of the most unattractive features of that model: the enhancement of hyperfine effects relative to spin-orbit effects[10,12] emerges automatically. The origin of this enhancement is threefold. One is simply that $\epsilon_{\rm cont}<\epsilon_{\rm so}$, and another is that there are cancellations between $V_{\rm so(cm)}$ and $V_{\rm so(TP)}$, but the main effect is a consequence of the fact that, with its attractive δ function, the hyperfine interaction produces effects which are much stronger than those one would obtain from lowest-order perturbation theory in $V_{\rm hyp}$. The physics of this important enhancement is sufficiently simple that it warrants explanation; we proceed by contrasting the hyperfine interaction in the light hadrons with that in the ground state of positronium. In either case if the δ function of the hyperfine interaction is left unsmeared the hyperfine splitting will be infinite. To see this consider a harmonic-oscillator variational wave function

$$\psi_0(r)=\frac{\beta^{3/2}}{\pi^{3/4}}e^{-\beta^2r^2/2}$$

for e^+e^- or $q\bar{q}$: upper bounds on the ground-state energies are (using for simplicity a pure Coulomb potential $-\alpha/r$ for e^+e^-, a pure linear potential br for $q\bar{q}$, and nonrelativistic kinematics in both cases)

$$E_0^{e^+e^-}(\beta)=\frac{3\beta^2}{2m_e}-\left[\frac{4}{\pi}\right]^{1/2}\alpha\beta-\left[\frac{4}{\pi}\right]^{1/2}\frac{\alpha\beta^3}{m_e{}^2}$$

and

$$E_0^{q\bar{q}}(\beta)=\frac{3\beta^2}{2m_q}+\left[\frac{4}{\pi}\right]^{1/2}\frac{b}{\beta}-\left[\frac{4}{\pi}\right]^{1/2}\frac{\frac{4}{3}\alpha_s\beta^3}{m_q{}^2}\ .$$

In both cases by taking $\beta\to\infty$ one finds that E_0 is unbounded from below. On the other hand, when the hyperfine interaction is smeared so that

$$\delta^3(\mathbf{r})\to\frac{\sigma^3}{\pi^{3/2}}e^{-\sigma^2r^2}\ ,$$

the β^3 appearing in the third terms above is replaced by $\beta^3\sigma^3/(\beta^2+\sigma^2)^{3/2}$ so that a true minimum occurs in each E_0 at a finite value of β. Since in the e^+e^- system α is very small and $\sigma\sim m_e\gg\beta\sim m_e\alpha$, one can easily check that the minimum of $E_0^{e^+e^-}$ occurs at a value that to an excellent approximation is shifted from its unperturbed value by the usual result of lowest-order perturbation theory. In the light-quark system, on the other hand, α_s is not small and $\sigma\sim\beta\sim m_q\sim\Lambda_{\rm QCD}$, so that the minimum is found at a value of β far from its unperturbed value, and the resulting $E_0^{q\bar{q}}$ lies considerably below the value one would calculate from lowest-order perturbation theory. This means that a smaller value of α_s (consistent with the small spin-orbit splittings seen in the light hadrons) can produce the large hyperfine splittings which are required in, e.g., ρ-π and Δ-N.

A second principal objective of this work was to test whether the description of both mesons and baryons could be unified in a single consistent framework. We have found that the relativized quark model of this work and Ref. 16 accomplishes this unification: as we have already mentioned, when we use *without any change* the meson-based parameters of Ref. 16 in our calculations, we obtain excellent results for all of the main features of baryon spectroscopy. Thus we find that the Δ-N splitting has a common origin to the ρ-π splitting (the hyperfine interaction), the $N^*(1520)\frac{1}{2}^-$-$N(940)\frac{1}{2}^+$ splitting has a common origin to the A_2-ρ splitting (an orbital excitation in the Coulomb plus linear potential), the Σ-Λ splitting has a common origin to the $(K^*-K)/(\rho-\pi)$ ratio (the mass dependence of hyperfine splittings), the $\Lambda\frac{5}{2}^-$-$\Sigma\frac{5}{2}^-$ splitting has a common origin to the $(f'-A_2)/(\phi-\rho)$ ratio (the mass dependence of orbital excitation energies), etc.

Table I introduced earlier shows the parameters that we actually used for baryon spectroscopy. After making the above observations using the parameters of Ref. 16 without change, we searched in parameter space for better solutions. As can be seen from Table I, we found that the meson-based parameters were optimal with the exception of the string tension and three of the ϵ parameters. It turns out that these three ϵ parameters (unlike the others) were not very tightly constrained by meson physics. The reason for this is simple: in baryons tensor and spin-orbit forces can cause mixing between states like $\Delta\,{}^4D_S\frac{5}{2}^+$ and $\Delta\,{}^2D_S\frac{5}{2}^+$ which are degenerate in the absence of spin-dependent effects (so that very large mixing angles can result from modest perturbations) while in mesons such mixings are almost always small since the relevant states are split by orbital excitation energy. It has, indeed, been verified[19] that the use of *our* ϵ's in meson spectroscopy leave the good results of Ref. 16 essentially unaltered. It is, furthermore, more natural to have our result $\epsilon_{\rm cont}\simeq\epsilon_{\rm tens}$ since these two terms arise from the same term in the reduction of one-gluon exchange (see Appendix A). On the other hand, the small decrease which we found useful in the string tension b (our high spin states were becoming increasingly too massive) is not readily accommodated by meson spectroscopy.[20] We assume that this small differ-

ence appears as a result of the neglect of nonadiabatic glue effects (or possibly mixing with higher Fock-space components) which can of course differ in mesons and baryons.

The spectroscopic results of our calculation are given in Tables III–XI and Figs. 3–14. In the tables we list all of the low-lying states predicted by the model; it will be noted that usually many more states are predicted than have been observed. In the usual nonrelativistic model there appears to be a good reason for this: analysis of the predicted strong-coupling amplitudes of the states of that model show an essentially one-to-one correspondence between states predicted to couple to their formation channels (πN for N's and Δ's and $\bar{K}N$ for Σ's and Λ's) and those observed.[21] To carry out a simple check of whether our calculation maintained these desirable features (without performing our own comprehensive decay analysis) we truncated our Hamiltonian matrices at the $N=2$ oscillator band to correspond to the calculations of Refs. 10 and 21. We then recalculated the hadronic couplings of our states to discover (using the criteria of Ref. 21) which of the many predicted states belonging to the $N=0$, 1, and 2 bands *ought* to have been seen. (In most cases the compositions were very similar to those of the usual nonrelativistic model of Ref. 10). These are the states shown in the figures as solid bars along with boxes representing the observed states, and indicated in the tables by an arrow. Clearly the observed correspondence is excellent (although there are some remaining problems). We will expand upon this comparison in the next section.

VI. A DETAILED COMPARISON BETWEEN THEORY AND EXPERIMENT

While studying Tables III–XI and Figs. 3–14 is sufficient to reach an appreciation of the general success of this model, a more detailed discussion is required to complete its comparison to experiment. In this section we will present such a discussion organized around the specific sectors of baryon spectroscopy displayed in those tables and figures. Spectroscopy on its own is a blunt tool, and one of the main purposes of our detailed discussion will be to point out the extent to which the predicted internal compositions of our model's states are in accord with measured strong and electromagnetic decay amplitudes. In doing this we will be using the analysis of Ref. 21 in the way described in Sec. V.

A. The ground-state baryons of SU(3)$_f$

The masses of the orbital ground-state baryons made of u, d, and s quarks are given in Table III and Fig. 3. The error in our extrapolation to $N_{\max}=\infty$ is about 20 MeV for these states, which is roughly represented by the width of the solid bars. We have already mentioned several features of these results, but we will nevertheless reemphasize here that the Δ-N splitting is a prediction based on the meson parameters of Ref. 16. This remarkable fact provides further evidence that, while the pion may sometimes be most economically viewed as the (almost) Goldstone boson of broken chiral symmetry, it may also usefully be viewed as the hyperfine partner of the ρ meson.

TABLE III. The ground-state baryons.

State, J^P	Predicted mass (MeV)	Experiment (MeV)
$N\frac{1}{2}^+$	960	939
$\Delta\frac{3}{2}^+$	1230	1232
$\Lambda\frac{1}{2}^+$	1115	1116
$\Sigma\frac{1}{2}^+$	1190	1193
$\Sigma\frac{3}{2}^+$	1370	1384
$\Xi\frac{1}{2}^+$	1305	1318
$\Xi\frac{3}{2}^+$	1505	1533
$\Omega\frac{3}{2}^+$	1635	1672

It seems to us that those who are willing to accept that the Δ-N splitting is due to color hyperfine interactions, but who nevertheless wish to accord the ρ-π splitting special status, are now left in an inconsistent position: these calculations indicate that splittings in "nonchiral" systems like Δ-N and in "chiral" systems like ρ-π have the same origin in terms of constituent quarks, even though they appear to be quite different in the current-quark basis. From Fig. 3 it appears that a slightly heavier s quark would improve our spectrum. While this is true in this case [a 5% increase in m_s would, e.g., correctly give the mass of the $\Omega(1672)$], we have found that such an increase would produce a deterioration of our excited-state spectra. Indeed, as previously mentioned, the Ref. 16 value for m_s seems to be globally optimal.

We next note that our calculations continue to support the original observation[22] that the Σ-Λ splitting is a hyperfine interaction effect: we get $(\Sigma-\Lambda)_{\text{theory}}=75\pm15$ MeV vs $(\Sigma-\Lambda)_{\text{expt}}\simeq 80$ MeV. (The theoretical error on the $N_{\max}\to\infty$ extrapolation of this mass difference is smaller than on either mass separately.) We also find $\Sigma^*-\Sigma=180\pm15$ MeV (vs 190 MeV) and $\Xi^*-\Xi=200\pm15$ MeV (vs 215 MeV). Thus, as in the usual nonrelativistic model,[10,11] the spectroscopy of the ground-state baryons is well described.

We have not yet begun a detailed analysis of such static properties as the magnetic moments, G_A/G_V, charge ra-

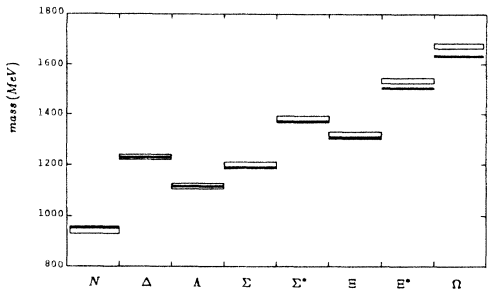

FIG. 3. The ground-state baryons.

TABLE IV. The negative-parity $S=0$ excited baryons. (a) States in the $N=1$ band. (b) Predictions for other states below 2200 MeV.

(a)

State, J^P	Predicted mass (MeV)	Experiment (MeV)	Status
$N^*\frac{1}{2}^-$	1460←	1520–1560	****
	1535←	1620–1680	****
$\Delta^*\frac{1}{2}^-$	1555←	1600–1650	****
$N^*\frac{3}{2}^-$	1495←	1510–1530	****
	1625←	1670–1730	***
$\Delta^*\frac{3}{2}^-$	1620←	1630–1740	****
$N^*\frac{5}{2}^-$	1630←	1660–1690	****

(b)

$N^*\frac{1}{2}^-$	1945,2030,2070,2145,2195
$\Delta^*\frac{1}{2}^-$	2035,2140
$N^*\frac{3}{2}^-$	1960,2055,2095,2165,2180
$\Delta^*\frac{3}{2}^-$	2080,2145
$N^*\frac{5}{2}^-$	2080,2095,2180
$\Delta^*\frac{5}{2}^-$	2155,2165
$N^*\frac{7}{2}^-$	2090

dii, etc., of these states. However, it seems likely that such an analysis will support the general picture of Ref. 15. For example, it was found there that relativistic corrections reduced G_A/G_V from the bad nonrelativistic value of $\frac{5}{3}$ to near its observed value. Another observation made in Ref. 15 was that the charge radius of a relativistic system was larger than the rms radius of its wave function by terms of order $1/m_q$. We expect that, as was found for mesons in Ref. 16, such terms account for what would otherwise be a discrepancy between the measured charge radii and the spatial extent of our quark-model wave functions. (This discrepancy is even greater in relativized models than it was in nonrelativistic quark models.)

B. The $S=0$ negative-parity baryons of the $N=1$ band

The masses of the $S=0$ negative-parity baryons below 2200 MeV are given in Table IV. Our model predicts the center of gravity of the $N=1$ band of such states to be about 50 MeV too low. We display in Fig. 4 our predictions for these states shifted upward by this modest discrepancy in order to show clearly that the pattern of splittings in this band is well predicted. The quality of these mass predictions as well as of the predicted strong couplings of these states is once again comparable to that of the nonrelativistic model of Ref. 10 (for which the center of gravity is essentially a free parameter). There is, however, one improvement here which is significant: we find that $\Delta^*\frac{3}{2}^- - \Delta^*\frac{1}{2}^- \simeq 70$ MeV (in agreement with the experimental indications) instead of the degeneracy of the usual nonrelativistic model.[10,12]

C. The $S=-1$ negative-parity baryons

The masses of the negative-parity Λ's and Σ's below 2300 MeV are given in Table V; Fig. 5 displays those states of the $N=1$ band which are predicted to couple significantly to $\bar{K}N \to (\Sigma^*, \Lambda^*) \to \bar{K}N, \Sigma\pi, \Lambda\pi$, shifted by the same 50 MeV as in Fig. 4.

The pattern here is still similar to the nonrelativistic model, but there has been one significant deterioration in the quality of the results. This deterioration can be traced to the fact that our model produces a smaller orbital split-

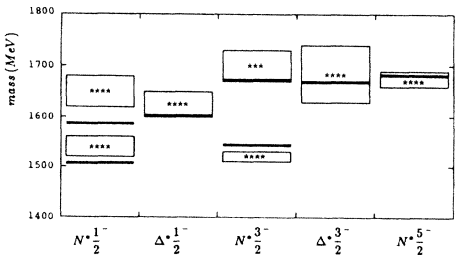

FIG. 4. The negative-parity $S=0$ excited baryons of the $N=1$ band: boxes show the experimental regions in which the resonances lie, bars show the predictions of the model for states that should be coupled, with $\Delta M = +50$ MeV.

TABLE V. The negative-parity $S=-1$ excited baryons. (a) States in the $N=1$ band. (b) Predictions for other states below 2300 MeV.

(a)

State, J^P	Predicted mass (MeV)	Experiment (MeV)	Status
$\Lambda^*\frac{1}{2}^-$	1550←	1400–1410	****
	1615←	1660–1680	****
	1675←	1720–1850	***
$\Sigma^*\frac{1}{2}^-$	1630←	1610–1635	**
	1675←	1730–1800	***
	1695		
$\Lambda^*\frac{3}{2}^-$	1545←	1520	****
	1645←	1685–1695	****
	1770		
$\Sigma^*\frac{3}{2}^-$	1655←	1665–1685	****
	1750←	1900–1950	***
	1755		
$\Lambda^*\frac{5}{2}^-$	1775←	1810–1830	****
$\Sigma^*\frac{5}{2}^-$	1755←	1770–1780	****

(b)

$\Lambda^*\frac{1}{2}^-$	2015,2095,2160,2195,2235,2280
$\Sigma^*\frac{1}{2}^-$	2110,2155,2165,2205,2260,2275
$\Lambda^*\frac{3}{2}^-$	2030,2110,2185,2230,2290
$\Sigma^*\frac{3}{2}^-$	2120,2185,2200,2215,2265,2290
$\Lambda^*\frac{5}{2}^-$	2180,2225,2240,2295
$\Sigma^*\frac{5}{2}^-$	2205,2250,2270,2280
$\Lambda^*\frac{7}{2}^-$	2150,2230
$\Sigma^*\frac{7}{2}^-$	2245

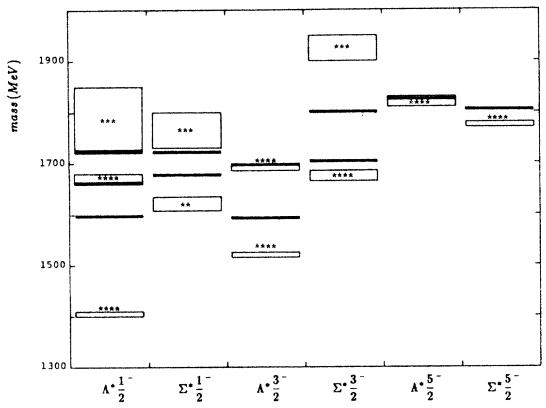

FIG. 5. The negative-parity $S=-1$ excited baryons of the $N=1$ band: legend as in Fig. 4.

ting between $L_\rho=1$ and $L_\lambda=1$ states than the nonrelativistic model of Ref. 10. The most prominent effect of this difference is that the lowest $\Lambda^*\frac{1}{2}^-$ state, which was already some 80 MeV too high in the nonrelativistic model of Ref. 10, is predicted to be nearly 150 MeV too high in our model. (Alternatively, one can note that it is still predicted to be nearly degenerate with the lowest $\Lambda^*\frac{3}{2}^-$ state,[10,12] while experimentally these states are split by over 100 MeV.) While this discrepancy must be considered very serious, its damage to the basic credibility of our model is, in our view, considerably tempered by the fact that the predicted internal compositions of all of these states [including the lowest $\Lambda^*\frac{1}{2}^-$ associated with the $\Lambda(1405)$] lead to quite good results for their decay amplitudes. Thus, in particular, the $\Lambda(1405)$ appears to be a dominantly $\chi^\rho\psi^\lambda$ state[23] as predicted. Our belief is therefore that the poorly predicted mass of this state does not point to a fundamental flaw in our model, but rather to the fact that effects outside of the scope of the model can occasionally be significant. In this case we believe that

the simplification we have made that is most likely faulty is our restriction to the qqq sector of Fock space. Indeed, the decay amplitude calculations just mentioned indicate that the lowest $\Lambda^*\frac{1}{2}^-$ state has an unusually large coupling to the $\bar{K}N$ channel, with respect to which it is an S-wave resonance. This coupling would naturally shift the predicted qqq state toward or even below $\bar{K}N$ threshold, which is where it is observed. At its observed mass the $\Lambda(1405)$ can decay only into $\Sigma\pi$, $\Lambda\gamma$, and $\Sigma\gamma$; one way to test whether it can be interpreted as a mass-shifted version of our uds state is to check, in addition to the known $\Sigma\pi$ amplitude, the two radiative decay amplitudes against those expected for our state.[24] Taken together these three measurements should be able to discriminate between the uds interpretation and alternatives like the old proposal that the $\Lambda(1405)$ is a $\bar{K}N$ bound state.[25]

D. The $S=0$ positive-parity baryons

The masses of the $S=0$ positive-parity baryons below 2200 MeV are given in Table VI, from which one can see that our model predicts the position of the center of gravity of the $N=2$ band of such states to be about 40 MeV too high. We have subtracted this modest overall error from our predictions for the $N=2$ band states to display the spectrum of Fig. 6. Recall that only states predicted to couple to πN (see Sec. V) are shown here; the remarkable success of the model is, we believe, quite evident from this picture. (For example, of the five $N^*\frac{3}{2}^+$ states predicted by the model, only the one which is observed is predicted to couple to πN, etc.) In this case the predictions of the relativized model are actually of higher quality than those of the usual nonrelativistic model. One example is that our lowest $N^*\frac{1}{2}^+$ state is predicted to couple to $N\pi$ more strongly than the next lowest; this is a reversal of the older predictions[21] which leads to results in better agreement with experiment. As another example we mention that the F to P ratio in the $\Delta\pi$ decays of the $\Delta^*\frac{5}{2}^+(1905)$ is now much greater than unity, bringing it into even better accord with experiment than the nonrelativistic model.[10,21] Nevertheless, though there are some improvements, it remains true that the character of the spectrum as well as the composition of the states is very similar to the predictions of the usual nonrelativistic model.

TABLE VI. The positive-parity $S=0$ excited baryons. (a) States in the $N=2$ band. (b) Predictions for other states below 2200 MeV.

State, J^P	Predicted mass (MeV)	Experiment (MeV)	Status
	(a)		
$N^*\frac{1}{2}^+$	1540←	1400–1480	****
	1770←	1680–1740	***
	1880		
	1975		
$\Delta^*\frac{1}{2}^+$	1835		
	1875←	1850–1950	****
$N^*\frac{3}{2}^+$	1795←	1690–1800	***
	1870		
	1910		
	1950		
	2030		
$\Delta^*\frac{3}{2}^+$	1795←	1520–1690	**
	1915←	1860–2060	***
	1985		
$N^*\frac{5}{2}^+$	1770←	1670–1690	****
	1980		
	1995←	1880–2030	**
$\Delta^*\frac{5}{2}^+$	1910←	1890–1920	****
	1990		
$N^*\frac{7}{2}^+$	2000←	1970–2020	**
$\Delta^*\frac{7}{2}^+$	1940←	1910–1960	****
	(b)		
$N^*\frac{1}{2}^+$	2065		

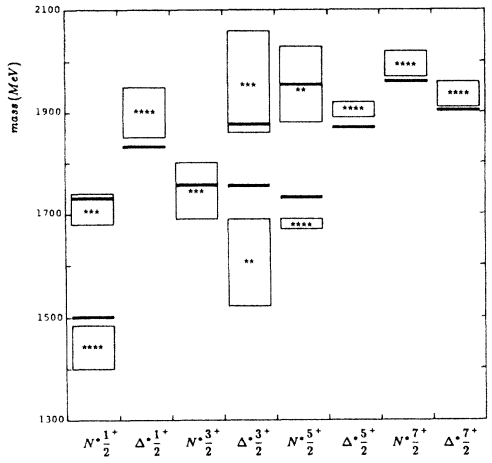

FIG. 6. The positive-parity $S=0$ excited baryons of the $N=2$ band: legend as in Fig. 4 but with $\Delta M=-40$ MeV.

Incidentally, on the basis of our calculations, we would conclude that the $N^*\frac{1}{2}^+(1440)$ (the Roper resonance) is not particularly problematical.[26] Of course our whole $N=2$ band appears about 40 MeV high, but if this is taken into consideration one sees that this state fits rather well into the pattern of Fig. 6.

E. The $S=-1$ positive-parity baryons

The predicted masses of the $S=-1$ positive-parity baryons below 2300 MeV are given in Table VII, while the spectrum of states in the $N=2$ band which couple (shifted as for their $S=0$ counterparts) is given in Fig. 7. These predictions are also similar to the nonrelativistic model of Ref. 10, but once again the quality is slightly improved.

TABLE VII. The positive-parity $S=-1$ excited baryons. (a) States in the $N=2$ band. (b) Predicted masses for other states below 2200 MeV.

(a)

State, J^P	Predicted mass (MeV)	Experiment (MeV)	Status
$\Lambda^*\frac{1}{2}^+$	1680←	1560–1700	* * *
	1830←, 1910←	1750–1850	* * *
	2010		
	2105		
	2120		
$\Sigma^*\frac{1}{2}^+$	1720←	1630–1690	* * *
	1915←, 1970←	1830–1985	* *
	2005		
	2030		
	2105		
$\Lambda^*\frac{3}{2}^+$	1900←	1850–1910	* * * *
	1960		
	1995		
	2050		
	2080		
	2120		
	2160		
$\Sigma^*\frac{3}{2}^+$	1920←	1800–1925	*
	1970		
	2010←	2070–2140	* *
	2030		
	2045		
	2085		
	2115		
	2155		
$\Lambda^*\frac{5}{2}^+$	1890←	1815–1825	* * * *
	2035←	2090–2140	* * *
	2115		
	2115		
	2180		
$\Sigma^*\frac{5}{2}^+$	1955←	1900–1935	* * * *
	2030←, 2095←	2010–2110	*
	2110		
	2130		
$\Lambda^*\frac{7}{2}^+$	2120←	2020–2120	*
$\Sigma^*\frac{7}{2}^+$	2060←	2025–2040	* * * *
	2125		

(b)

$\Lambda^*\frac{1}{2}^+$	2195,2270
$\Sigma^*\frac{1}{2}^+$	2240

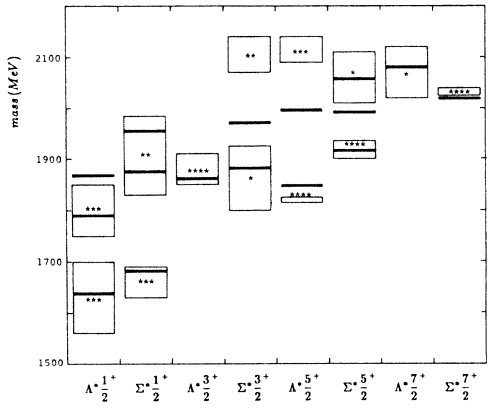

FIG. 7. The positive-parity $S=-1$ excited baryons of the $N=2$ band: legend as in Fig. 6.

One example is our prediction of two strongly coupled $\Lambda^*\frac{5}{2}^+$ states as observed (instead of one[21]).

F. $S=-2$ and -3 baryons

Our predictions for Ξ baryons below 2400 MeV and for Ω baryons below 2500 MeV are given in Table VIII, and the spectrum of states in the $N=0$, 1, and 2 bands is given in Figs. 8 and 9. In these cases there is no formation channel, so we show all states up to $N=2$ in the figures (using the same shifts as for their $S=0$ and -1 counterparts). There is little experimental information available at the moment, so these results are for the most part predictions. (Note that the actual predictions of the model are given in the tables, but we consider our best predictions for the location of the states up to $N=2$ to be those given in the figures, where we have corrected for the known errors of the model in predicting the center of gravity of the bands.)

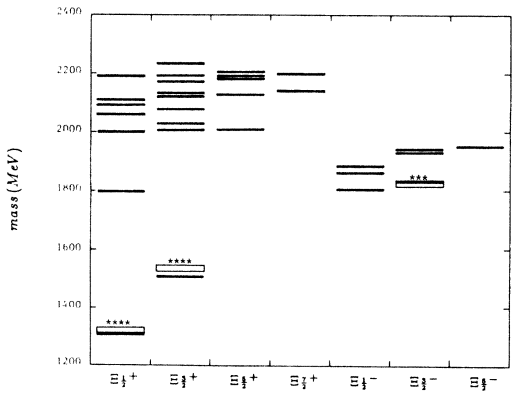

FIG. 8. The Ξ baryons up to $N=2$: we have applied $\Delta M=+50$ MeV to the negative-parity excited states and $\Delta M=-40$ MeV to the positive-parity excited states. Note that the $\Xi(1820)$ is reported to have spin-$\frac{3}{2}$ but its parity is unknown. Since it fits naturally into the spectrum if we assign a negative parity, we assume it has $J^P=\frac{3}{2}^-$.

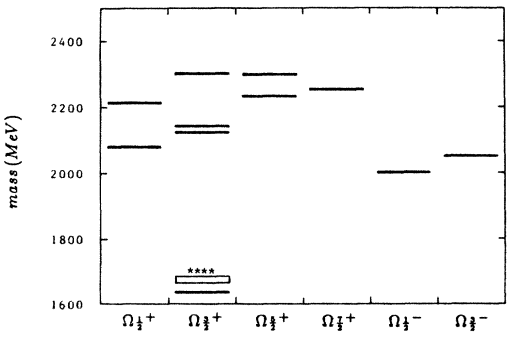

FIG. 9. The Ω baryons up to $N=2$: legend as in Fig. 8.

G. Other baryons made of *u*, *d*, and *s* quarks

In Table IX and Fig. 10 we show the lowest-lying states of $S=0$ baryons with J^P from $\frac{1}{2}^{\pm}$ to $\frac{11}{2}^{\pm}$. Since these (Regge-trajectory-type) sequences of states correspond to systems with increasingly large separations, these results support our *qqq* confinement mechanism. A similarly successful plot exists for high spin mesons[20] based on Ref. 16.

The experimental states shown in Figs. 3–10 in fact nearly exhaust the known well-established baryon resonances. There are, however, a few other well-established states. Most fit well into our model. However, one, the $\Delta^*\frac{5}{2}^-$ with mass 1930±30 MeV, has an interesting and controversial history. It appears to be considerably too low in mass to belong to the $N=3$ band, and on this basis it was suggested that it might be a hybrid baryon (i.e., a gluonic excitation).[27] Later, it was noted[28] that in the usual nonrelativistic treatment the $[56,1^-]$ SU(6) supermultiplet to which this state is naturally assigned automatically splits off from the $N=3$ band to become the lowest lying supermultiplet of the $N=3$ band (much as the $[56,0^+]$ to which the controversial $N\frac{1}{2}^+(1440)$ belongs splits off from the $N=2$ band to become the lowest lying SU(6) supermultiplet of $N=2$—see Sec. VI D). It was then accordingly argued that this was probably an ordinary $[56,1^-]$ state. Our calculation does little to resolve this controversy: we predict this state to be at 2030 MeV, rather far above its observed mass. On the other hand, we know that while our model is good at predicting the pattern of a spectrum, it can easily miss predicting the absolute mass of a state by 50 MeV, and sometimes miss by more.

Our tentative conclusion is that there is no compelling evidence for the existence of any baryon which does not fit into our model. We do not, therefore, hold out much hope for models of hybrid baryons which predict many new states in the 1.5–2.0-GeV region.[29] A corollary is that we expect that it will be very difficult in the near fu-

TABLE VIII. The Ξ and Ω baryons below 2400 and 2500 MeV, respectively.

State, J^P	Predicted masses (MeV)							
$\Xi\frac{1}{2}^+$	1305							
$\Xi\frac{3}{2}^+$	1505							
$\Xi^*\frac{1}{2}^-$	1755	1810	1835	2225	2285	2300	2320	2380
$\Xi^*\frac{3}{2}^-$	1785	1880	1895	2240	2305	2330	2340	2385
$\Xi^*\frac{5}{2}^-$	1900	2345	2350	2385				
$\Xi^*\frac{7}{2}^-$	2355							
$\Xi^*\frac{1}{2}^+$	1840	2040	2100	2130	2150	2230	2345	
$\Xi^*\frac{3}{2}^+$	2045	2065	2115	2165	2170	2210	2230	2275
$\Xi^*\frac{5}{2}^+$	2045	2165	2230	2230	2240			
$\Xi^*\frac{7}{2}^+$	2180	2240						
$\Omega\frac{3}{2}^+$	1635							
$\Omega^*\frac{1}{2}^-$	1950	2410	2490					
$\Omega^*\frac{3}{2}^-$	2000	2440	2495					
$\Omega^*\frac{5}{2}^-$	2490							
$\Omega^*\frac{1}{2}^+$	2220	2255						
$\Omega^*\frac{3}{2}^+$	2165	2280	2345					
$\Omega^*\frac{5}{2}^+$	2280	2345						
$\Omega^*\frac{7}{2}^+$	2295							

TABLE IX. The $S=0$ baryons versus spin-parity.

State, J^P	Predicted mass (MeV)	Experiment (MeV)	Status
$N\frac{1}{2}^+$	960	939	****
$\Delta\frac{3}{2}^+$	1230	1232	****
$N^*\frac{5}{2}^+$	1770	1670–1690	****
$\Delta^*\frac{7}{2}^+$	1940	1910–1960	****
$N^*\frac{9}{2}^+$	2345	2150–2300	****
$\Delta^*\frac{11}{2}^+$	2450	2380–2450	****
$N^*\frac{1}{2}^-$	1460	1520–1560	****
$N^*\frac{3}{2}^-$	1495	1510–1530	****
$N^*\frac{5}{2}^-$	1630	1660–1690	****
$N^*\frac{7}{2}^-$	2090 2205 2255 2305 2355	2120–2230	****
$N^*\frac{9}{2}^-$	2215	2130–2270	****
$N^*\frac{11}{2}^-$	2600 2670 2700 2770	2580–2700	***

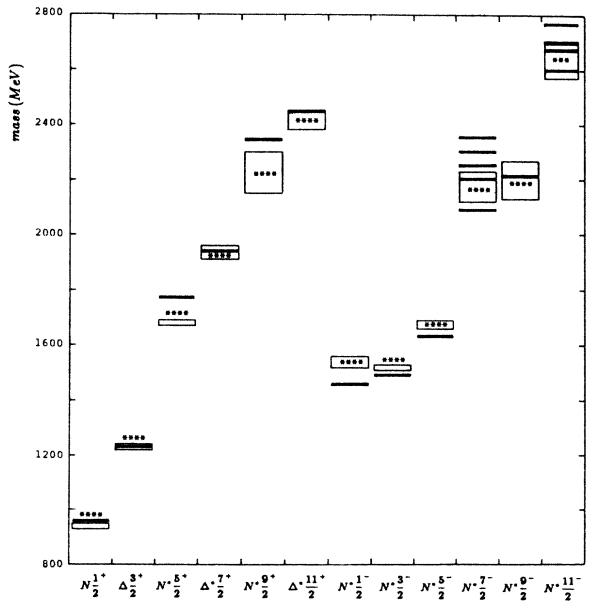

FIG. 10. The $S=0$ baryons plotted against spin-parity: boxes show the experimental regions in which the lowest energy resonances lie, bars show the states predicted by the model for each spin-parity.

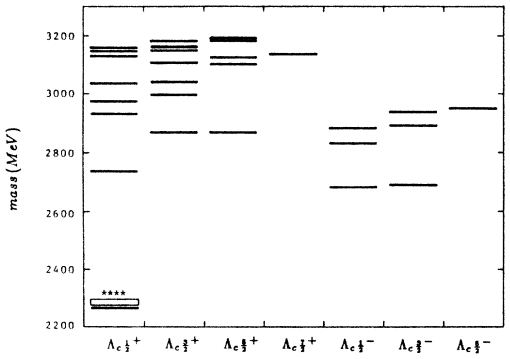

FIG. 11. The Λ_c baryons up to $N=2$: legend as in Fig. 8.

ture to identify hybrid baryons: they do not have exotic quantum numbers like some hybrid mesons do, and if indeed they are to be found only above 2 GeV (as predicted by some models[13] and indicated by the above observations) then it will be extremely difficult to disentangle them from the very rich structure of ordinary baryons expected in this mass range.

H. Charmed baryons

Table X shows our predictions for the charmed baryons below 3300 MeV, and Figs. 11 and 12 show our states in the $N=0$, 1, and 2 bands. There are two predictions here which can be compared to experiment at the moment. One is the prediction of the absolute mass of the $\Lambda_c\frac{1}{2}^+$ to within 20 MeV based on a charmed-quark mass taken from meson spectroscopy. We would argue that this is a nontrivial accomplishment of the model (recall that various authors have used charm-quark masses ranging from 1.2 to 1.9 GeV). We also predict that $\Sigma_c\frac{1}{2}^+ - \Lambda_c\frac{1}{2}^+ = 175\pm15$ MeV, which compares favorably to the experimental result of 166 ± 1 MeV. Our other predictions must await further data. (As with the $S=-2$ and -3 baryons, while our model predicts the masses

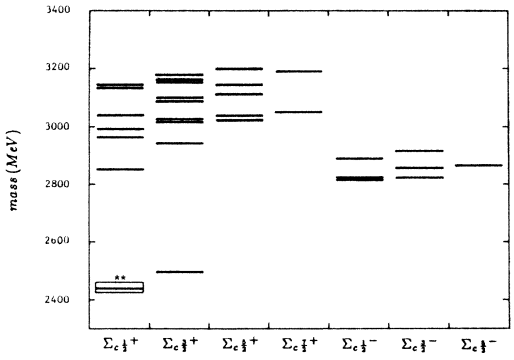

FIG. 12. The Σ_c baryons up to $N=2$: legend as in Fig. 8.

TABLE X. The Λ_c and Σ_c baryons.

State, J^P	Predicted masses (MeV)							
$\Lambda_c \frac{1}{2}^+$	2265							
$\Lambda_c^* \frac{1}{2}^-$	2630	2780	2830	3030	3200	3240	3255	
$\Lambda_c^* \frac{3}{2}^-$	2640	2840	2885	3035	3240	3255	3290	
$\Lambda_c^* \frac{5}{2}^-$	2900	3130	3275					
$\Lambda_c^* \frac{7}{2}^-$	3125							
$\Lambda_c^* \frac{1}{2}^+$	2775	2970	3015	3075	3170	3185	3200	
$\Lambda_c^* \frac{3}{2}^+$	2910	3035	3080	3145	3190	3200	3220	
$\Lambda_c^* \frac{5}{2}^+$	2910	3140	3165	3225	3230			
$\Lambda_c^* \frac{7}{2}^+$	3175							
$\Sigma_c \frac{1}{2}^+$	2440							
$\Sigma_c \frac{3}{2}^+$	2495							
$\Sigma_c^* \frac{1}{2}^-$	2765	2770	2840	3185	3195	3250	3290	
$\Sigma_c^* \frac{3}{2}^-$	2770	2805	2865	3195	3210	3260	3285	
$\Sigma_c^* \frac{5}{2}^-$	2815	3220	3280	3295				
$\Sigma_c^* \frac{7}{2}^-$	3290							
$\Sigma_c^* \frac{1}{2}^+$	2890	3005	3035	3080	3175	3185		
$\Sigma_c^* \frac{3}{2}^+$	2985	3060	3065	3130	3140	3200	3200	3220
$\Sigma_c^* \frac{5}{2}^+$	3065	3080	3155	3185	3240			
$\Sigma_c^* \frac{7}{2}^+$	3090	3230						

shown in the tables, we consider our best predictions for the locations of states up to $N=2$ to be those shown in the figures which have allowed for the known errors in the model's prediction of the center of gravity of the various bands.)

I. *b*-flavored baryons

Our predictions for the *b*-flavored baryons below 6600 MeV are given in Table XI, and Figs. 13 and 14 show our states in the $N=0$, 1, and 2 bands. We expect our absolute prediction of the mass of the $\Lambda_b \frac{1}{2}^+$ and $\Sigma_b \frac{1}{2}^+$ to be good to about 50 MeV. Note that our predicted $\Lambda_b \frac{1}{2}^+$ is consistent with the state claimed at 5425^{+175}_{-75} MeV.

J. Other heavy baryons

Our methods of solution are not well suited to baryons of the type *csu* (Ref. 30). We hope to be able to report on

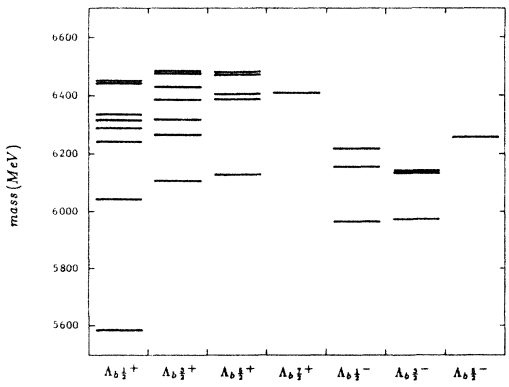

FIG. 13. The Λ_b baryons up to $N=2$: legend as in Fig. 8.

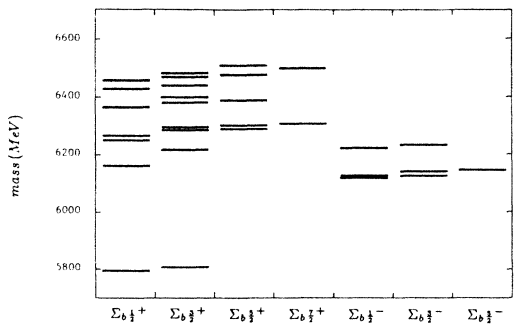

FIG. 14. The Σ_b baryons up to $N=2$: legend as in Fig. 8.

TABLE XI. The Λ_b and Σ_b baryons.

State, J^P	Predicted masses (MeV)							
$\Lambda_b \frac{1}{2}^+$	5585							
$\Lambda_b^* \frac{1}{2}^-$	5912	6100	6165	6260	6470	6500	6530	
$\Lambda_b^* \frac{3}{2}^-$	5920	6185	6190	6265	6510	6525	6540	6560
$\Lambda_b^* \frac{5}{2}^-$	6205	6360	6520	6565				
$\Lambda_b^* \frac{7}{2}^-$	6360							
$\Lambda_b^* \frac{1}{2}^+$	6045	6280	6330	6355	6375	6480	6485	
$\Lambda_b^* \frac{3}{2}^+$	6145	6305	6355	6425	6470	6515	6515	6520
$\Lambda_b^* \frac{5}{2}^+$	6165	6425	6440	6510	6510	6525		
$\Lambda_b^* \frac{7}{2}^+$	6445	6580						
$\Lambda_b^* \frac{9}{2}^+$	6580							
$\Sigma_b \frac{1}{2}^+$	5795							
$\Sigma_b \frac{3}{2}^+$	5805							
$\Sigma_b^* \frac{1}{2}^-$	6070	6070	6170	6440	6445	6510	6590	6590
$\Sigma_b^* \frac{3}{2}^-$	6070	6085	6180	6445	6455	6510	6525	6570
$\Sigma_b^* \frac{5}{2}^-$	6090	6460	6510	6535				
$\Sigma_b^* \frac{7}{2}^-$	6525	6525						
$\Sigma_b^* \frac{9}{2}^-$	6540							
$\Sigma_b^* \frac{1}{2}^+$	6200	6290	6300	6400	6465	6495	6575	
$\Sigma_b^* \frac{3}{2}^+$	6250	6320	6330	6415	6435	6475	6505	6520
$\Sigma_b^* \frac{5}{2}^+$	6325	6335	6420	6510	6545			
$\Sigma_b^* \frac{7}{2}^+$	6340	6535						

such baryons, as well as "doubly and triply heavy" baryons in the future.

VII. CONCLUSIONS AND FINAL COMMENTS

There is still much which remains to be done before drawing firm conclusions regarding this model. In particular, a more thorough study of the strong couplings of these states (preferably in either the flux-tube breaking[31] or naive pair-creation models[32]) is required. One would also like to study the (relativized) photodecay amplitudes, weak-current matrix elements, charge radii, etc., to see if the indications of Ref. 15, that these will improve the quark model, are borne out.

It would also be worthwhile to try to improve the model. The most urgently required improvement would be to show that the "relativistic ignorance parameters" σ_0, s, and the ϵ's are a good representation of the underlying physics or, alternatively, to replace the cutoff and momentum dependence they represent by more realistic forms. More fundamental studies are also required to answer the following questions: What are the effects of higher sectors of Fock space like $|q^4\bar{q}\rangle$? How does the adiabatic treatment of the glue implicit in the quark potential model break down? (One way which already seems clear from Ref. 14 and which may be responsible for some of the shortcomings of our model is the neglect of the contribution of the glue to moments of inertia.)

Even with such questions outstanding, we believe that the results presented here, especially when viewed in conjunction with the meson results of Ref. 16, are very significant. They provide powerful evidence that the naive quark-potential model can be placed on a much firmer footing within the context of QCD field theory. From this perspective the quark model appears to be the approximate low-energy effective theory based on cutting off QCD field theory to produce a picture of relativistic constituent quarks moving in the lowest adiabatic surfaces (i.e., static potentials) of the gluonic fields. While all of the aspects of this picture played a role in the work described here (and in Ref. 16), our main contribution is, of course, to show that the assumption of nonrelativistic dynamics was never an essential feature of the quark model and, indeed, that it was responsible for many of the inconsistencies of the usual approach.

In particular, we note that when taken together with the results of Ref. 16 on mesons, we have shown that all of meson and baryon spectroscopy and long-distance structure can be unified in a single framework (i.e., with a single Hamiltonian) which is consistent with our present understanding of QCD. This picture uses the stringlike picture of confinement, a universal value for $\alpha_s(r)$, a universal set of quark masses, the same one-gluon-exchange potentials for all sectors, etc.

Of course the resulting picture is not QCD. For example, it ignores mixing with gluonic excitations and violations of the truncations to the $q\bar{q}$ and qqq sectors of Fock space, and it contains the relativistic ignorance parameters

which can at best be considered rough imitations of the true physics. For all of these reasons, the model should not be (and is not) very accurate. Nevertheless, we believe that in view of these present limitations the results are entirely satisfactory. Our conclusion is that the mesons and baryons can for now be considered a reasonably well understood "background" to the new physics of the gluonic degrees of freedom of QCD. We also believe that it is now entirely appropriate to remove the derogatory "nonrelativistic" prefix from the quark potential model.

ACKNOWLEDGMENTS

This work owes a great deal to Ted Barnes, Steve Godfrey, David Kotchan, and Rick Kokoski at Toronto who all engaged in active discussions of the ongoing work. Our computations would not have been possible without the CPU time made available to us by George Luste and Anna Pezacki. This research was supported in part by grants from the Natural Sciences and Engineering Research Council of Canada. One of us (S.C.) would like to thank the Canadian Association of University Teachers for their support.

APPENDIX A: THE RELATIVIZED HAMILTONIAN FOR BARYONS

The Hamiltonian that we use for the baryon system is of the form

$$H = H_0 + V_{\rm oge} + V_{\rm conf} , \tag{A1}$$

where H_0 is a relativistic kinetic energy term:

$$H_0 = \sum_{i=1}^{3} (p_i^2 + m_i^2)^{1/2} , \tag{A2}$$

$V_{\rm oge}$ is a one-gluon-exchange potential which in the nonrelativistic limit goes to the usual Breit-Fermi interaction of Sec. III, and $V_{\rm conf}$ consists of a string potential and a spin-orbit term arising from this potential via Thomas precession. In this appendix we will explain the origin of these terms and give their precise form.

The mesonic analogues of the effective potentials we use in (A1) and the motivation behind them has been given in Ref. 16. It is argued there that the $p/m \to 0$ (Breit-Fermi) limit given in Eqs. (5)—(12) of the text will be modified by several effects.

(1) For qq scattering in the center-of-mass frame one can define an effective potential $V_{\rm eff}$ by

$$\chi^\dagger_{s_2'}\chi^\dagger_{s_1'} V_{\rm eff}(\mathbf{P},\mathbf{r})\chi_{s_1}\chi_{s_2} \equiv \frac{1}{(2\pi)^3}\int d^3Q\, e^{i\mathbf{Q}\cdot\mathbf{r}}\bar{u}(p_2's_2')\bar{u}(p_1's_1')I(Q^2)u(p_1s_1)u(p_2s_2) , \tag{A3}$$

where $\mathbf{Q}\equiv\mathbf{p}_1'-\mathbf{p}_1$ and $\mathbf{P}\equiv\frac{1}{2}(\mathbf{p}_1'+\mathbf{p}_1)$, and where $I(Q^2)$ is the effective exchange propagator of the interaction [e.g., $I(Q^2)=G(Q^2)(\gamma^\mu)_1 g_{\mu\nu}(\gamma^\nu)_2$ defined in (A9) below for the one-gluon-exchange interaction]. For *on-shell* qq scattering $V_{\rm eff}$ will reproduce all matrix elements exactly. We note, however, that the momentum dependence of the spinors will introduce $\mathbf{Q}$ dependence [which will become $\mathbf{r}$ dependence via (A3)] and $\mathbf{P}$ dependence (which makes $V_{\rm eff}$ nonlocal) not seen in the $p_i/m_i \to 0$ limit. Since we are interested in situations where at least some p_i/m_i are of order unity, we must take the possibility of such modifications seriously. Very roughly speaking, the message of these modifications is that when p_i is comparable to m_i, then there is an $m \leftrightarrow E$ ambiguity in the Breit-Fermi potentials. For example, the hyperfine interaction one obtains from the above prescription is not that of the Breit-Fermi interaction but rather, with

$$G(\mathbf{r}) \equiv (2\pi)^{-3}\int d^3Q\, e^{i\mathbf{Q}\cdot\mathbf{r}} G(Q^2)$$

but taking the $Q^2 \to 0$ limit of the other factors,

$$\chi^\dagger_{s_2'}\chi^\dagger_{s_1'}\left[\frac{m_1 m_2}{E_1 E_2}\right](\delta_{rs}\delta_{uv}-\delta_{rv}\delta_{su})\frac{S_{1r}S_{2s}}{m_1 m_2} \times \nabla_u\nabla_v G(r_{12})\chi_{s_1}\chi_{s_2} . \tag{A4}$$

which differs precisely by the replacement of the m_i in (9) by E_i.

(2) While one can always write the Schrödinger equation (1), in a field theory it must be interpreted with some care. In the first place, the state $|\psi\rangle$ will in general be a superposition of states from different sectors of Fock space, and indeed in an interacting theory with ultraviolet cutoff μ sent to infinity, the coefficients of each term in such an expansion will vanish. Thus a constituent picture (of hadrons or even atoms) only makes sense if the field theory is cut off at some finite scale μ. Ideally, one chooses μ to be sufficiently large that the phenomena of interest are not sensitive to physics of scales greater than μ, but sufficiently small that the Fock-space expansion is rapidly converging. Finally, to obtain a Schrödinger equation for the valence sector of Fock space, one can integrate out the higher components of Fock space, replacing their effects by an effective potential. From this discussion we discover two more modifications we must in general expect in the Breit-Fermi interaction: (a) the constituent quarks are not pointlike, but rather will have a graininess appropriate to the scale μ, and (b) since the quarks are in general off-shell, the potential which arises from this procedure will be a modification of the one obtained from (A3).

In view of these observations, following Ref. 16, we first introduce a quark smearing function

$$\rho_{ij}(\mathbf{r}-\mathbf{r}') = \frac{\sigma_{ij}^3}{\pi^{3/2}} e^{-\sigma_{ij}^2(\mathbf{r}-\mathbf{r}')^2} \tag{A5}$$

for the interaction of quarks i and j which parametrizes some of the effects of the cutoff μ and of the nonlocalities and Q dependence expected for r around the quark Compton wavelength. We apply this smearing to all of the two-body potentials $V(r)$ of the nonrelativistic limit to obtain smeared potentials $\tilde{V}(r)$ according to

$$\tilde{V}_{ij}(r) = \int d^3r'\rho_{ij}(\mathbf{r}-\mathbf{r}')V_{ij}(\mathbf{r}') \tag{A6}$$

with the Ref. 16 prescription that

$$\sigma_{ij}{}^2=\sigma_0{}^2\left[\frac{1}{2}+\frac{1}{2}\left[\frac{4m_im_j}{(m_i+m_j)^2}\right]^4\right]+s^2\left[\frac{2m_im_j}{m_i+m_j}\right]^2, \tag{A7}$$

where σ_0 and s are the parameters given in Table I. (Baryons are not as sensitive to σ_{ij} as mesons and a simpler form would have sufficed for us, but we adopt this result from Ref. 16 without any change for the sake of universality. Note that its main features are that for $m\equiv m_i=m_j\to\infty$, σ_{ij} is proportional to m and for $m\to 0$, σ_{ij} goes to a constant characteristic of the scale of chiral-symmetry breaking.) Note that upon Fourier transforming (A6) we have simply

$$\tilde{V}_{ij}(Q^2)=\rho_{ij}(Q^2)V_{ij}(Q^2)\ . \tag{A8}$$

The second modification we make to the potentials of the nonrelativistic limit is to allow them to take on explicit momentum dependence. As the arguments above indicate, we cannot expect to be able to read off the correct momentum dependence from the on-shell relativistic scattering amplitudes; however, we use these amplitudes to motivate the form of the modifications which we assume. For example, on the basis of (A4) we assume that the fully modified hyperfine interaction has the form (13) of the text, reproduced as Eq. (A17) below.

We would now like to complete this appendix by giving the explicit forms of each of the potentials we use in our calculation. Before presenting this catalog, however, we must describe how we treat the running coupling constant $\alpha_s(Q^2)$ which appears in the one-gluon-exchange kernel:

$$G(Q^2)\equiv-\tfrac{2}{3}\alpha_s(Q^2)\frac{4\pi}{Q^2}\ . \tag{A9}$$

With N_f flavors with masses much less than Q^2, in lowest order

$$\alpha_s(Q^2)=\frac{12\pi}{(33-2N_f)\ln(Q^2/\Lambda_{\rm QCD}{}^2)}\ , \tag{A10}$$

as given earlier in Eq. (15). As $Q^2\to\Lambda_{\rm QCD}{}^2$ this lowest-order formula diverges, a behavior which we associate with the onset of confinement. We accordingly assume that as $Q^2\to 0$ we should take $\alpha_s(Q^2)$ to saturate at some value $\alpha_s^{\rm critical}$ since the physics of the divergent behavior of (A10) has been taken into account in the linear confining potential. We also allow for "thresholds" by taking N_f in (A10) to be the number of flavors with $4m_f{}^2<Q^2$ while demanding that "$\Lambda_{\rm QCD}$" in (A10) varies so that α_s will be continuous. We take *the* $\Lambda_{\rm QCD}$ to refer explicitly to the $N_f=2$ region of Q^2 evolution. We then parametrize this theoretical $\alpha_s(Q^2)$ curve based on (A10) with $\Lambda_{\rm QCD}=200$ MeV to the more convenient form given in Eq. (16) of the text where $\alpha_s^{\rm critical}$ of Eq. (17) is the only free parameter [the other parameters in (16) are being used simply to describe the theoretical curve: see Fig. 2]. The functional form (16) is convenient because, as we will see immediately, it is easily convoluted with the relativistic smearing (A8), and easily integrated against our harmonic-oscillator basis functions.

We are finally in a position to present our effective potentials. The one-gluon-exchange propagator (A9) is, with the functional forms chosen, easily smeared with (A5) to give

$$\tilde{G}(r_{ij})=-\sum_k\frac{2\alpha_k}{3r_{ij}}\mathrm{erf}(\sigma_{kij}r_{ij})\ , \tag{A11}$$

where

$$\sigma_{kij}{}^{-2}=\gamma_k{}^{-2}+\sigma_{ij}{}^{-2}\ . \tag{A12}$$

All of the one-gluon-exchange potentials can now be expressed in terms of $\tilde{G}(r_{ij})$. In each case, following the mesonic case of Ref. 16, we have taken the on-shell amplitude obtained from $\tilde{G}(Q^2)$ via (A3) as a starting point, but allowed for the on-shell momentum dependence to be modified. Thus we take

$$V_{\rm oge}=\sum_{i<j}V_{ij}^{\rm oge} \tag{A13}$$

with

$$V_{ij}^{\rm oge}=V_{ij}^{\rm Coul}+V_{ij}^{\rm hyp}+V_{ij}^{{\rm so}(v)} \tag{A14}$$

where

$$V_{ij}^{\rm Coul}=(\beta_{ij})^{1/2+\epsilon_{\rm Coul}}\tilde{G}(r_{ij})(\beta_{ij})^{1/2+\epsilon_{\rm Coul}}\ , \tag{A15}$$

$$V_{ij}^{\rm hyp}=V_{ij}^{\rm cont}+V_{ij}^{\rm tens}\ , \tag{A16}$$

with

$$V_{ij}^{\rm cont}=(\delta_{ij})^{1/2+\epsilon_{\rm cont}}\frac{2\mathbf{S}_i\cdot\mathbf{S}_j}{3m_im_j}\nabla^2\tilde{G}(r_{ij})(\delta_{ij})^{1/2+\epsilon_{\rm cont}}\ , \tag{A17}$$

$$V_{ij}^{\rm tens}=(\delta_{ij})^{1/2+\epsilon_{\rm tens}}\frac{1}{3m_im_j}\left[\frac{3\mathbf{S}_i\cdot\mathbf{r}_{ij}\mathbf{S}_j\cdot\mathbf{r}_{ij}}{r_{ij}{}^2}-\mathbf{S}_i\cdot\mathbf{S}_j\right]\left[\frac{1}{r_{ij}}\frac{d\tilde{G}(r_{ij})}{dr_{ij}}-\frac{d^2\tilde{G}(r_{ij})}{dr_{ij}{}^2}\right](\delta_{ij})^{1/2+\epsilon_{\rm tens}}\ , \tag{A18}$$

and

$$V_{ij}^{{\rm so}(v)}=\frac{1}{r_{ij}}\frac{d\tilde{G}(r_{ij})}{dr_{ij}}\left[(\delta_{ii})^{1/2+\epsilon_{{\rm so}(v)}}\frac{\mathbf{r}_{ij}\times\mathbf{p}_i\cdot\mathbf{S}_i}{2m_i{}^2}(\delta_{ii})^{1/2+\epsilon_{{\rm so}(v)}}-(\delta_{jj})^{1/2+\epsilon_{{\rm so}(v)}}\frac{\mathbf{r}_{ij}\times\mathbf{p}_j\cdot\mathbf{S}_j}{2m_j{}^2}(\delta_{jj})^{1/2+\epsilon_{{\rm so}(v)}}\right.$$

$$\left.-(\delta_{ij})^{1/2+\epsilon_{{\rm so}(v)}}\frac{\mathbf{r}_{ij}\times\mathbf{p}_j\cdot\mathbf{S}_i-\mathbf{r}_{ij}\times\mathbf{p}_i\cdot\mathbf{S}_j}{m_im_j}(\delta_{ij})^{1/2+\epsilon_{{\rm so}(v)}}\right]\ , \tag{A19}$$

where

$$\beta_{ij}=1+\frac{{p_{ij}}^2}{({p_{ij}}^2+{m_i}^2)^{1/2}({p_{ij}}^2+{m_j}^2)^{1/2}} \tag{A20}$$

and

$$\delta_{ij}=\frac{m_i m_j}{({p_{ij}}^2+{m_i}^2)^{1/2}({p_{ij}}^2+{m_j}^2)^{1/2}}\ , \tag{A21}$$

where p_{ij} is the magnitude of the momentum of either of the quarks in the ij center-of-mass frame, and the ϵ's are free parameters designed to allow the rough description of a momentum dependence more general than that of the on-shell amplitudes (A3). It should be noted that for simplicity we have ignored the "second-order spin-orbit" terms of the form

$$(\mathbf{Q}\cdot\mathbf{P}\times\mathbf{S}_1)\cdot(\mathbf{Q}\cdot\mathbf{P}\times\mathbf{S}_2)\tilde{G}(Q^2)$$

since the first-order terms are already quite small.

Finally, we turn to the confinement potential $V_{\rm conf}$ in (A1) which consists of a string potential and its associated spin-orbit term from Thomas precession. In the limit of slowly moving quarks, the string picture suggests[13,33,34] that, apart from an overall constant, there will be an adiabatic potential corresponding to the energy of the minimum length of the Y string configuration (see Fig. 1). There is a simple rule for finding the position of the junction of the three strings which accomplishes this minimization: if any one of the angles in the triangle made by connecting the quarks is greater than 120° then the junction point is on top of the quark which lies at the vertex of that angle; otherwise the junction is at the unique point which makes the arms of the Y shaped string at 120° to each other. The string potential in terms of ρ, λ, and $\cos\theta=(\boldsymbol{\rho}\cdot\boldsymbol{\lambda})/\rho\lambda$, is then

$$V_{\rm string}=C_{qqq}+b\begin{cases}(\frac{3}{2})^{1/2}[\rho^2+\lambda^2+2\rho\lambda(1-\cos^2\theta)^{1/2}]^{1/2} & \text{if all angles } \theta_{ijk}<120^\circ\ ,\\ r_{12}+r_{13}, & \theta_{312}>120^\circ\ ,\\ r_{12}+r_{23}, & \theta_{123}>120^\circ\ ,\\ r_{13}+r_{23}, & \theta_{132}>120^\circ\ ,\end{cases} \tag{A22}$$

where C_{qqq} is an overall constant energy shift and

$$r_{12}=\sqrt{2}\rho\ , \tag{A23}$$

$$r_{13}=\frac{1}{\sqrt{2}}(\rho^2+3\lambda^2+2\sqrt{3}\rho\lambda\cos\theta)^{1/2}\ , \tag{A24}$$

$$r_{23}=\frac{1}{\sqrt{2}}(\rho^2+3\lambda^2-2\sqrt{3}\rho\lambda\cos\theta)^{1/2}\ . \tag{A25}$$

We have found it convenient to break $V_{\rm string}$ up into an effective two-body piece and a three-body piece:

$$V_{\rm string}=C_{qqq}+fb\sum_{i<j}r_{ij}+V_{3b} \tag{A26}$$

where

$$V_{3b}=b\left[\sum_{i=1}^{3}|\mathbf{r}_i-\mathbf{r}_{\rm junction}|-f\sum_{i<j}r_{ij}\right]\ , \tag{A27}$$

with $f=0.5493$ (see Ref. 34) chosen to minimize the size of the expectation value of V_{3b} in the harmonic-oscillator ground state of the baryon system. We can then treat the two-body part of $V_{\rm string}$ exactly and compute the (always small) corrections due to V_{3b} perturbatively. (Note that this means that $V_{\rm string}$ is quite close to the potential $\sum_{i<j}\frac{1}{2}br_{ij}$ one would obtain from the $\mathbf{F}_i\cdot\mathbf{F}_j$ potential model of confinement.[7])

The above result for $V_{\rm string}$ is analogous to the result (A9) for $V_{\rm oge}$; we expect it to be modified by smearing and relativistic corrections. For the smearing we proceed as usual using (A5) to obtain $\tilde{V}_{\rm string}$ from $V_{\rm string}$ [we ignore the effect of smearing on the small three-body terms so that (A8) can be applied directly]. The relativistic corrections are more problematical. Gromes has shown[35] that in leading order the spin-dependent terms associated with the confining potential are identical to those arising from scalar exchange, i.e., a pure Thomas precession. We thus take

$$V_{\rm so(s)}=\sum_{i<J}V_{ij}^{\rm so(s)} \tag{A28}$$

with

$$V_{ij}^{\rm so(s)}=\frac{1}{r_{ij}}\frac{\partial\tilde{V}_{\rm string}}{\partial r_{ij}}\left[(\delta_{ii})^{1/2+\epsilon_{\rm so(s)}}\frac{\mathbf{r}_{ij}\times\mathbf{p}_i\cdot\mathbf{S}_i}{2{m_i}^2}(\delta_{ii})^{1/2+\epsilon_{\rm so(s)}}-(\delta_{jj})^{1/2+\epsilon_{\rm so(s)}}\frac{\mathbf{r}_{ij}\times\mathbf{p}_j\cdot\mathbf{S}_j}{2{m_j}^2}(\delta_{jj})^{1/2+\epsilon_{\rm so(s)}}\right]\ . \tag{A29}$$

On the basis of the solutions to the at least superficially similar example of QED in one dimension,[36] we assume that $\tilde{V}_{\rm string}$ is unmodified by momentum-dependent factors. In Ref. 16 it was shown that meson phenomenology constrains any such modifications to be very small.

APPENDIX B: EVALUATION OF MATRIX ELEMENTS

In Sec. IV we discussed the general outline of the calculation of matrix elements. We also discussed techniques for dealing with the H_{13} and H_{23} matrix elements, and

with the momentum-dependent factors in the Hamiltonian. Here we show how to obtain matrix elements of the various pieces of the Hamiltonian.

1. The Coulomb and two-body string energies

The Coulomb and two-body string energies [see (A15) and (A26)] are terms which are scalar in space and independent of spin. If we evaluate, for example, the matrix element $\langle\alpha|\tilde{G}(r_{12})|\beta\rangle$, with $|\alpha\rangle$ and $|\beta\rangle$ given by (27) (with the same JM), we see that since $\tilde{G}(r_{12})$ only depends on $r_{12}=\sqrt{2}\rho$, the λ integration will be zero unless the two spatial wave functions Ψ^α and Ψ^β have identical $\boldsymbol{\lambda}$ oscillator wave functions, and that the ρ integration is zero unless the two spatial wave functions have identical l_ρ values. Furthermore, since the interaction is an overall spin and space scalar, the entire matrix element is zero unless the spin wave functions are identical and unless the total orbital angular momenta are equal. If we adopt the notation

$$|nl\rangle=\alpha^{3/2}\mathcal{N}_{nl}(\alpha r)^l e^{-\alpha^2r^2/2}L_n^{l+1/2}(\alpha r) \tag{B1}$$

then

$$\langle n_{\rho_\alpha}l_{\rho_\alpha}|V(\sqrt{2}\rho)|n_{\rho_\beta}l_{\rho_\beta}\rangle=\mathcal{N}_{n_{\rho_\alpha}l_{\rho_\alpha}}\mathcal{N}_{n_{\rho_\beta}l_{\rho_\beta}}\alpha^3\int_0^\infty\rho^2d\rho\,e^{-\alpha^2\rho^2}(\alpha\rho)^{l_{\rho_\alpha}+l_{\rho_\beta}}L_{n_{\rho_\alpha}}^{l_{\rho_\alpha}+1/2}(\sqrt{2}\alpha\rho)V(\sqrt{2}\rho)\times L_{n_{\rho_\beta}}^{l_{\rho_\beta}+1/2}(\sqrt{2}\alpha\rho)\,, \tag{B2}$$

and we may write

$$\langle\alpha|\tilde{G}(r_{12})|\beta\rangle=\delta_{S_\alpha S_\beta}\delta_{L_\alpha L_\beta}\delta_{l_{\rho_\alpha}l_{\rho_\beta}}\delta_{n_{\lambda_\alpha}n_{\lambda_\beta}}\delta_{l_{\lambda_\alpha}l_{\lambda_\beta}}\langle n_{\rho_\alpha}l_{\rho_\alpha}|\tilde{G}(\sqrt{2}\rho)|n_{\rho_\beta}l_{\rho_\alpha}\rangle\,. \tag{B3}$$

Note that S_α represents both the type and total spin of the spin wave function of the state $|\alpha\rangle$. The analogous equation holds for the matrix element of the effective two-body string potential with $\tilde{G}$ replaced by $\tilde{V}_{\text{string}}$.

2. The hyperfine contact term

The hyperfine contact energy $\tilde{V}_{12}^{\text{cont}}(r_{12})$ is an example of a scalar operator which is simultaneously scalar in both space and spin. Its expectation value breaks up into a product of a radial integral and a spin matrix element:

$$\langle\alpha|\tilde{V}_{12}^{\text{cont}}(r_{12})|\beta\rangle=\delta_{L_\alpha L_\beta}\delta_{l_{\rho_\alpha}l_{\rho_\beta}}\delta_{n_{\lambda_\alpha}n_{\lambda_\beta}}\delta_{l_{\lambda_\alpha}l_{\lambda_\beta}}\times\left\langle n_{\rho_\alpha}l_{\rho_\alpha}\left|\sum_k\frac{2\alpha_k}{3m_1m_2}\frac{8\pi}{3}\frac{\sigma_{k12}{}^3}{\pi^{3/2}}e^{-2\sigma_{k12}{}^2\rho^2}\right|n_{\rho_\beta}l_{\rho_\beta}\right\rangle\langle S_\alpha m|\mathbf{S}_1\cdot\mathbf{S}_2|S_\beta m\rangle\,, \tag{B4}$$

where the above holds for any m and we have suppressed the momentum dependence in (A17) for the time being. The spin matrix elements are very simple, the only nonzero matrix elements being

$$\langle\chi_{1/2,m}^{M_\rho}|\mathbf{S}_1\cdot\mathbf{S}_2|\chi_{1/2,m}^{M_\rho}\rangle=-\tfrac{3}{4}\,, \tag{B5}$$

$$\langle\chi_{1/2,m}^{M_\lambda}|\mathbf{S}_1\cdot\mathbf{S}_2|\chi_{1/2,m}^{M_\lambda}\rangle=\tfrac{1}{4}\,, \tag{B6}$$

$$\langle\chi_{3/2,m}^{S}|\mathbf{S}_1\cdot\mathbf{S}_2|\chi_{3/2,m}^{S}\rangle=\tfrac{1}{4}\,. \tag{B7}$$

3. The hyperfine tensor interaction

The tensor terms [see (A18)] are evaluated with the aid of the Wigner-Eckhart theorem, which is applied twice: once to the scalar product of the spin-tensor and spatial-tensor operators which make up this term in the Hamiltonian, and then again to the $L=2$ tensor operator which is to be evaluated in a basis made up from coupling l_ρ and l_λ to give $\mathbf{L}$. First we write [again we suppress the momentum dependence in (A18) for the time being]

$$\tilde{V}_{12}^{\text{tens}}=\tilde{V}^t(\sqrt{2}\rho)\mathbf{R}_2(12)\cdot\mathbf{S}_2(12)\,, \tag{B8}$$

where

$$\mathbf{R}_2(12)=\begin{pmatrix}\frac{\sqrt{3}}{2}\hat{r}_+{}^2\\ -\sqrt{3}\hat{r}_+\hat{r}_z\\ \vdots\\ \frac{\sqrt{3}}{2}\hat{r}_-{}^2\end{pmatrix}\,, \tag{B9}$$

$$\mathbf{S}_2(12)=\begin{bmatrix} \frac{\sqrt{3}}{2}S_{1+}S_{2+} \\ -\sqrt{3}(S_{1+}S_{2z}+S_{1z}S_{2+}) \\ \vdots \\ \frac{\sqrt{3}}{2}S_{1-}S_{2-} \end{bmatrix}, \tag{B10}$$

and where from (A18)

$$\tilde{V}^t(\sqrt{2}\rho)=\sum_k \frac{2\alpha_k}{3m_1m_2}\left[\frac{\mathrm{erf}(\sqrt{2}\sigma_{k12}\rho)}{2\sqrt{2}\rho^3}-\frac{4\pi}{3}\frac{{\sigma_{k12}}^3}{\pi^{3/2}}e^{-2{\sigma_{k12}}^2\rho^2}\left[1+\frac{3}{4{\sigma_{k12}}^2\rho^2}\right]\right]. \tag{B11}$$

Then we apply the Wigner-Eckhart theorem to the tensor product $\tilde{V}_{12}^{\mathrm{tens}}$ to obtain

$$\begin{aligned}\langle\alpha\,|\,\tilde{V}_{12}^{\mathrm{tens}}\,|\,\beta\rangle=&(-1)^{J-L_\alpha-S_\beta}W(L_\alpha L_\beta S_\alpha S_\beta;2J)\sqrt{2L_\alpha+1}\sqrt{2S_\alpha+1}\\ &\times\langle L_\alpha n_{\rho_\alpha}l_{\rho_\alpha}n_{\lambda_\alpha}l_{\lambda_\alpha}||\tilde{V}^t(\sqrt{2}\rho)\mathbf{R}_2(12)||L_\beta n_{\rho_\beta}l_{\rho_\beta}n_{\lambda_\beta}l_{\lambda_\beta}\rangle\langle S_\alpha||\mathbf{S}_2(12)||S_\beta\rangle\,.\end{aligned} \tag{B12}$$

The theorem is applied again to the spatial reduced matrix element

$$\begin{aligned}\langle L_\alpha n_{\rho_\alpha}l_{\rho_\alpha}n_{\lambda_\alpha}l_{\lambda_\alpha}||\tilde{V}^t(\sqrt{2}\rho)\mathbf{R}_2(12)||L_\beta n_{\rho_\beta}l_{\rho_\beta}n_{\lambda_\beta}l_{\lambda_\beta}\rangle=&(-1)^{L_\alpha+l_{\rho_\beta}-2-l_{\lambda_\alpha}}W(l_{\rho_\alpha}l_{\rho_\beta}L_\alpha L_\beta;2l_{\lambda_\alpha})\\ &\times\langle n_{\rho_\alpha}l_{\rho_\alpha}||\tilde{V}^t(\sqrt{2}\rho)\mathbf{R}_2(12)||n_{\rho_\beta}l_{\rho_\beta}\rangle\delta_{n_{\lambda_\alpha}n_{\lambda_\beta}}\delta_{l_{\lambda_\alpha}l_{\lambda_\beta}}\,.\end{aligned} \tag{B13}$$

The spin and space reduced matrix elements appearing in (B12) and (B13), respectively, are

$$\langle S_\alpha||\mathbf{S}_2(12)||S_\beta\rangle=\begin{bmatrix} (\frac{5}{8})^{1/2} & 0 & (\frac{5}{8})^{1/2} \\ 0 & 0 & 0 \\ -\frac{\sqrt{5}}{2} & 0 & 0 \end{bmatrix}, \tag{B14}$$

where the ijth entry in the matrix corresponds to $\langle\chi_i||\mathbf{S}_2(12)||\chi_j\rangle$, with $\chi_1=\chi^S_{3/2}$, $\chi_2=\chi^\rho_{1/2}$, and $\chi_3=\chi^\lambda_{1/2}$, and

$$\langle n_{\rho_\alpha}l_{\rho_\alpha}||\tilde{V}^t(\sqrt{2}\rho)\mathbf{R}_2(12)||n_{\rho_\beta}l_{\rho_\beta}\rangle=C(l_{\rho_\beta}200;l_{\rho_\alpha}0)\left[\frac{2(2l_{\rho_\beta}+1)}{2l_{\rho_\alpha}+1}\right]^{1/2}\langle n_{\rho_\alpha}l_{\rho_\alpha}\,|\,\tilde{V}^t(\sqrt{2}\rho)\,|\,n_{\rho_\beta}l_{\rho_\beta}\rangle\,. \tag{B15}$$

4. The spin-orbit interactions

If we apply the baryon center-of-momentum frame identities

$$\mathbf{p}_1=\frac{1}{\sqrt{2}}\mathbf{p}_\rho+\frac{1}{\sqrt{6}}\mathbf{p}_\lambda\,, \tag{B16}$$

$$\mathbf{p}_2=-\frac{1}{\sqrt{2}}\mathbf{p}_\rho+\frac{1}{\sqrt{6}}\mathbf{p}_\lambda\,, \tag{B17}$$

$$\mathbf{p}_3=-\frac{2}{\sqrt{6}}\mathbf{p}_\lambda\,, \tag{B18}$$

to the spin-orbit potentials (A19) and (A29) we obtain [because of the unusual dependence of the spin-orbit effect on the quark masses, we show both the (12) and (13) potentials]

$$V_{12}^{\mathrm{so}}=\frac{1}{2\sqrt{2}\rho}\frac{d\tilde{V}(r_{12})}{dr_{12}}\left[\frac{(4g-1)}{{m_1}^2}(\mathbf{S}_1+\mathbf{S}_2)\cdot\boldsymbol{l}_\rho-\frac{1}{{m_1}^2}(\mathbf{S}_1-\mathbf{S}_2)\cdot\frac{1}{\sqrt{3}}\boldsymbol{\rho}\times\mathbf{p}_\lambda\right], \tag{B19}$$

$$V_{13}^{\rm so}=\frac{1}{2\sqrt{2}\rho'}\frac{d\tilde{V}(r_{13})}{dr_{13}}\left[\frac{2g-1}{{m_1}^2}\left[\mathbf{S}_1\cdot\boldsymbol{l}_{\rho'}+\mathbf{S}_1\cdot\frac{1}{\sqrt{3}}\boldsymbol{\rho}'\times\mathbf{p}_{\lambda'}\right]+\frac{2g-1}{{m_3}^2}\left[\mathbf{S}_3\cdot\boldsymbol{l}_{\rho'}-\mathbf{S}_3\cdot\frac{1}{\sqrt{3}}\boldsymbol{\rho}'\times\mathbf{p}_{\lambda'}\right]\right.$$
$$\left.+\frac{2g}{m_1m_3}\left[(\mathbf{S}_1+\mathbf{S}_3)\cdot\boldsymbol{l}_{\rho'}-(\mathbf{S}_1-\mathbf{S}_3)\cdot\frac{1}{\sqrt{3}}\boldsymbol{\rho}'\times\mathbf{p}_{\lambda'}\right]\right], \tag{B20}$$

where $g=1$ and $\tilde{V}=\tilde{G}$ for the one-gluon-exchange potential, and $g=0$ and $\tilde{V}=\tilde{V}_{\rm string}$ for the spin-orbit potential from confinement. The terms proportional to $\boldsymbol{\rho}\times\mathbf{p}_\lambda$ and $\boldsymbol{\rho}'\times\mathbf{p}_{\lambda'}$ are the three-body spin-orbit potentials. These can be understood[37] as consequences of the Wigner rotation which occurs when boosting from the center-of-mass frame of the baryon to the center-of-mass frame of quarks i and j. They must be dealt with specially, because they are of a completely different form than the rest of the operators dealt with so far. Let us write a general (12) spin-orbit potential [a similar form holds with different mass dependencies for the (13) potentials in the primed frame] in the form

$$\frac{1}{2\sqrt{2}m_1m_2}\frac{F(\rho)}{\rho}\left[c_1\mathbf{S}_{2b}\cdot\boldsymbol{l}_\rho+c_2\mathbf{S}_{3b}\cdot\frac{1}{\sqrt{3}}\boldsymbol{\rho}\times\mathbf{p}_\lambda\right], \tag{B21}$$

where c_1 and c_2 are constants, and where $\mathbf{S}_{2b}$ and $\mathbf{S}_{3b}$ are of the form $a\mathbf{S}_1+b\mathbf{S}_2$. Then we may apply the Wigner-Eckhart theorem to the spin-space scalar product to obtain

$$\langle\alpha\,|\,\tilde{V}_{12}^{\rm so}\,|\,\beta\rangle=\frac{1}{2\sqrt{2}m_1m_2}(-1)^{J-L_\alpha-S_\beta}W(L_\alpha L_\beta S_\alpha S_\beta;1J)\sqrt{2L_\alpha+1}\sqrt{2S_\alpha+1}$$
$$\times\left[c_1\left\langle L_\alpha n_{\rho_\alpha}l_{\rho_\alpha}n_{\lambda_\alpha}l_{\lambda_\alpha}\left|\left|\frac{F(\rho)}{\rho}l_\rho\right|\right|L_\beta n_{\rho_\beta}l_{\rho_\beta}n_{\lambda_\beta}l_{\lambda_\beta}\right\rangle\langle S_\alpha||\mathbf{S}_{2b}||S_\beta\rangle\right.$$
$$\left.+c_2\left\langle L_\alpha n_{\rho_\alpha}l_{\rho_\alpha}n_{\lambda_\alpha}l_{\lambda_\alpha}\left|\left|\frac{F(\rho)}{\rho}\frac{1}{\sqrt{3}}\boldsymbol{\rho}\times\mathbf{p}_\lambda\right|\right|L_\beta n_{\rho_\beta}l_{\rho_\beta}n_{\lambda_\beta}l_{\lambda_\beta}\right\rangle\langle S_\alpha||\mathbf{S}_{3b}||S_\beta\rangle\right]. \tag{B22}$$

We may then apply the theorem again to the spatial reduced matrix elements

$$\left\langle L_\alpha n_{\rho_\alpha}l_{\rho_\alpha}n_{\lambda_\alpha}l_{\lambda_\alpha}\left|\left|\frac{F(\rho)}{\rho}l_\rho\right|\right|L_\beta n_{\rho_\beta}l_{\rho_\beta}n_{\lambda_\beta}l_{\lambda_\beta}\right\rangle=(-1)^{L_\alpha+l_{\rho_\alpha}-1-l_{\lambda_\alpha}}W(l_{\rho_\alpha}l_{\rho_\beta}L_\alpha L_\beta;1l_{\lambda\alpha})$$
$$\times[(2L_\beta+1)l_{\rho_\alpha}(l_{\rho_\alpha}+1)(2l_{\rho_\alpha}+1)]^{1/2}$$
$$\times\delta_{l_{\rho_\alpha}l_{\rho_\beta}}\delta_{n_{\lambda_\alpha}n_{\lambda_\beta}}\delta_{l_{\lambda_\alpha}l_{\lambda_\beta}}\left\langle n_{\rho_\alpha}l_{\rho_\alpha}\left|\frac{F(\rho)}{\rho}\right|n_{\rho_\beta}l_{\rho_\beta}\right\rangle, \tag{B23}$$

and

$$\left\langle L_\alpha n_{\rho_\alpha}l_{\rho_\alpha}n_{\lambda_\alpha}l_{\lambda_\alpha}\left|\left|\frac{F(\rho)}{\rho}\frac{1}{\sqrt{3}}\boldsymbol{\rho}\times\mathbf{p}_\lambda\right|\right|L_\beta n_{\rho_\alpha}l_{\rho_\beta}n_{\rho_\beta}l_{\lambda_\beta}\right\rangle$$
$$=[(2L_\beta+1)(2l_{\rho_\alpha}+1)(2l_{\lambda_\alpha}+1)]^{1/2}X\begin{pmatrix}L_\alpha & L_\beta & 1\\ l_{\rho_\alpha} & l_{\rho_\beta} & 1\\ l_{\lambda_\alpha} & l_{\lambda_\beta} & 1\end{pmatrix}C(l_{\rho_\alpha}100;l_{\rho_\beta}0)$$
$$\times(-i)^{(2n_{\lambda_\alpha}+l_{\lambda_\alpha})-(2n_{\lambda_\beta}+l_{\lambda_\beta})}C(l_{\lambda_\alpha}100;l_{\lambda_\beta}0)\langle n_{\rho_\alpha}l_{\rho_\alpha}\,|\,F(\rho)\,|\,n_{\rho_\beta}l_{\rho_\beta}\rangle\langle n_{\lambda_\alpha}l_{\lambda_\alpha}\,|\,\lambda\,|\,n_{\lambda_\beta}l_{\lambda_\beta}\rangle, \tag{B24}$$

where X is a 9-j coefficient. The spin reduced matrix elements appearing (B22) are

$$\langle S_\alpha||a\mathbf{S}_1+b\mathbf{S}_2||S_\beta\rangle=\begin{pmatrix}\frac{1}{2}(\frac{5}{3})^{1/2}(a+b) & \frac{1}{2}(a-b) & \frac{1}{2\sqrt{3}}(a+b)\\ -\frac{1}{\sqrt{2}}(a-b) & 0 & -\frac{1}{2}(a-b)\\ -\frac{1}{\sqrt{6}}(a+b) & -\frac{1}{2}(a-b) & \frac{1}{\sqrt{3}}(a+b)\end{pmatrix}, \tag{B25}$$

where the ijth entry in the matrix corresponds to $\langle \chi_i || a\mathbf{S}_1 + b\mathbf{S}_2 || \chi_j \rangle$, with the χ_i as in (B14).

5. The three-body string energy

We saw above that V_{string} can be simply expressed in terms of ρ, λ, and $\cos\theta = \boldsymbol{\rho}\cdot\boldsymbol{\lambda}/\rho\lambda$. Similarly the effective two-body string potential can be written down in terms of these variables. We now form the function $V_{3b}(\rho,\lambda,\cos\theta)$ from V_{string} by subtracting $fb\sum_{i<j} r_{ij}$ [see (A27)]. Our task is to find the matrix element $\langle \alpha \mid V_{3b} \mid \beta \rangle$. First, we evaluate the angular integral (the Clebsch-Gordan sums required to couple the ρ and λ angular momenta are suppressed for simplicity)

$$\int d\Omega_\rho d\Omega_\lambda Y^*_{l_{\rho_\alpha} m_{\rho_\alpha}}(\Omega_\rho) Y^*_{l_{\lambda_\alpha} m_{\lambda_\alpha}}(\Omega_\lambda) V_{3b}(\rho,\lambda,\cos\theta) Y_{l_{\rho_\beta} m_{\rho_\beta}}(\Omega_\rho) Y_{l_{\lambda_\beta} m_{\lambda_\beta}}(\Omega_\lambda) \, . \tag{B26}$$

This is accomplished by rewriting the product of the two $Y(\Omega_\rho)$'s as a sum over a single $Y_{L_\rho M_\rho}(\Omega_\rho)$, and similarly for the $Y(\Omega_\lambda)$'s. Then we note that the angle θ is the angle of the $\boldsymbol{\lambda}$ vector with respect to the $\boldsymbol{\rho}$ vector, and that we may perform the $d\Omega_\lambda$ integral if we first rotate the $Y(\Omega_\lambda)$ into the coordinate frame where $\boldsymbol{\rho}$ lies along the z axis, using the relation

$$Y_{L_\lambda M_\lambda}(\Omega_\lambda) = \sum_N Y_{L_\lambda N}(\Omega^\rho_\lambda) D^{L_\lambda}_{N M_\lambda}(-R) \, , \tag{B27}$$

where D is a rotation matrix, R is the rotation with Euler angles ϕ_ρ, θ_ρ, and $-\phi_\rho$, and $\Omega^\rho_\lambda = (\theta,\phi^\rho_\lambda)$ is the angular position of $\boldsymbol{\lambda}$ with respect to $\boldsymbol{\rho}$. The resulting $d\Omega^\rho_\lambda$ integral is proportional to

$$\delta_{N0} V_{L_\lambda}(\rho,\lambda) = \delta_{N0} \int_0^1 d\cos\theta P_{L_\lambda}(\cos\theta) V_{3b}(\rho,\lambda,\cos\theta) \, , \tag{B28}$$

where P_{L_λ} is a Laguerre polynomial. Carrying out the sum over N, we find that the D matrix turns into a $Y(\Omega_\rho)$, which may then be integrated against the remaining $Y_{L_\rho M_\rho}(\Omega_\rho)$ to yield

$$\begin{aligned}
&(-1)^{l_{\rho_\alpha} - l_{\lambda_\alpha} + l_{\rho_\beta} - l_{\lambda_\beta}} (2L+1)[(2l_{\rho_\alpha}+1)(2l_{\rho_\beta}+1)(2l_{\lambda_\alpha}+1)(2l_{\lambda_\beta}+1)]^{1/2} \\
&\quad \times \sum_{m_{\rho_\alpha} m_{\lambda_\alpha}} \sum_{m_{\rho_\beta} m_{\lambda_\beta}} (-1)^{m_{\rho_\alpha} + m_{\lambda_\alpha}} \begin{pmatrix} l_{\rho_\alpha} & l_{\lambda_\alpha} & L \\ m_{\rho_\alpha} & m_{\lambda_\alpha} & M \end{pmatrix} \begin{pmatrix} l_{\rho_\beta} & l_{\lambda_\beta} & L \\ m_{\rho_\beta} & m_{\lambda_\beta} & M \end{pmatrix} \\
&\quad \times \sum_{L_\rho M_\rho} (2L_\rho + 1)(-1)^{M_\rho} \begin{pmatrix} l_{\rho_\alpha} & l_{\rho_\beta} & L_\rho \\ -m_{\rho_\alpha} & m_{\rho_\beta} & -M_\rho \end{pmatrix} \begin{pmatrix} l_{\lambda_\alpha} & l_{\lambda_\beta} & L_\rho \\ -m_{\lambda_\alpha} & m_{\lambda_\beta} & M_\rho \end{pmatrix} \\
&\quad \times \begin{pmatrix} l_{\rho_\alpha} & l_{\rho_\beta} & L_\rho \\ 0 & 0 & 0 \end{pmatrix} \begin{pmatrix} l_{\lambda_\alpha} & l_{\lambda_\beta} & L_\rho \\ 0 & 0 & 0 \end{pmatrix} V_{L_\rho}(\rho,\lambda) \, ,
\end{aligned} \tag{B29}$$

where $\mid LM \rangle$ is the orbital angular momentum of both $\mid \alpha \rangle$ and $\mid \beta \rangle$, and we have written all Clebsch-Gordan coefficients in terms of the 3-j coefficients for clarity. The next step is to identify the sum over the magnetic quantum numbers as a Racah coefficient and restore the radial integrations which results in (after some algebra)

$$\begin{aligned}
\langle \alpha \mid V_{3b} \mid \beta \rangle &= \delta_{S_\alpha S_\beta} \delta_{L_\alpha L_\beta} [(2l_{\rho_\alpha}+1)(2l_{\rho_\beta}+1)(2l_{\lambda_\alpha}+1)(2l_{\lambda_\beta}+1)]^{1/2} (-1)^{L + l_{\lambda_\alpha} + l_{\lambda_\beta}} \\
&\quad \times \sum_{L_\rho} C(l_{\rho_\alpha} 0 l_{\rho_\beta} 0; L_\rho 0) C(l_{\lambda_\alpha} 0 l_{\lambda_\beta} 0; L_\rho 0) W(l_{\rho_\alpha} l_{\rho_\beta} l_{\lambda_\alpha} l_{\lambda_\beta}; L_\rho L) \\
&\quad \times \langle n_{\rho_\alpha} l_{\rho_\alpha} \mid \langle n_{\lambda_\alpha} l_{\lambda_\alpha} \mid V_{L_\rho}(\rho,\lambda) \mid n_{\lambda_\beta} l_{\lambda_\beta} \rangle \mid n_{\rho_\beta} l_{\rho_\beta} \rangle \, ,
\end{aligned} \tag{B30}$$

where the last line is the obvious generalization of the radial integral in (B2). The $\cos\theta$ integrals in (B28) and the ρ and λ integrals in (B30) can be carried out numerically.

6. Momentum-dependent terms

It remains to discuss how we deal with the momentum dependence of various terms in H. The center-of-momentum frame formulas (B16)—(B18) indicate that the way to proceed with the kinetic energy is to evaluate the matrix element

$\langle\alpha|(p_3^2+m_3^2)^{1/2}|\beta\rangle$ in the ρ,λ basis, since there $\mathbf{p}_3$ is just proportional to $\mathbf{p}_\lambda$. Then we may note that since $|\alpha\rangle$ and $|\beta\rangle$ are antisymmetric under exchange of quarks one and two

$$\langle\alpha|(p_1^2+m_1^2)^{1/2}|\beta\rangle=\langle\alpha|(p_2^2+m_1^2)^{1/2}|\beta\rangle\ , \tag{B31}$$

and these matrix elements are best evaluated in the ρ',λ' basis, where $\mathbf{p}_2=-(2/\sqrt{6})\mathbf{p}_{\lambda'}$. Then we have that

$$\langle\alpha|(p_3^2+m_3^2)^{1/2}|\beta\rangle=\delta_{S_\alpha S_\beta}\delta_{L_\alpha L_\beta}\delta_{n_{\rho_\alpha}n_{\rho_\beta}}\delta_{l_{\rho_\alpha}l_{\rho_\beta}}\delta_{l_{\lambda_\alpha}l_{\lambda_\beta}}\langle n_{\lambda_\alpha}l_{\lambda_\alpha}|(\tfrac{2}{3}p_\lambda^2+m_3^2)^{1/2}|n_{\lambda_\beta}l_{\lambda_\beta}\rangle\ . \tag{B32}$$

Using the relation between the Fourier transform of a harmonic-oscillator wave function and itself [see Eq. (39)], we find

$$\langle n_{\lambda_\alpha}l_{\lambda_\alpha}|(\tfrac{2}{3}p_\lambda^2+m_3^2)^{1/2}|n_{\lambda_\beta}l_{\lambda_\beta}\rangle=(-i)^{-N_\alpha+N_\beta}\langle n_{\lambda_\alpha}l_{\lambda_\alpha}|(\tfrac{2}{3}\lambda^2+m_3^2)^{1/2}|n_{\lambda_\beta}l_{\lambda_\beta}\rangle_{1/\alpha}\ , \tag{B33}$$

where

$$\langle n_{\lambda_\alpha}l_{\lambda_\alpha}|V(\lambda)|n_{\lambda_\beta}l_{\lambda_\beta}\rangle_{1/\alpha}=\mathcal{N}_{n_{\lambda_\alpha}l_{\lambda_\alpha}}\mathcal{N}_{n_{\lambda_\beta}l_{\lambda_\beta}}\frac{1}{\alpha^3}\int_0^\infty\lambda^2 d\lambda\, e^{-\lambda^2/\alpha^2}(\lambda/\alpha)^{l_{\lambda_\alpha}+l_{\lambda_\beta}}L_{n_{\lambda_\alpha}}^{l_{\lambda_\alpha}+1/2}(\sqrt{2}\lambda/\alpha)$$
$$\times V(\lambda)L_{n_{\lambda_\beta}}^{l_{\lambda\beta}+1/2}(\sqrt{2}\lambda/\alpha)\ . \tag{B34}$$

The calculation of the matrix elements of the momentum-dependent factors in (A15)—(A29) is made simpler by the ansatz that the momentum appearing in the (ij) factor is $\mathbf{p}_{ij(cm)}=(\mathbf{p}_i-\mathbf{p}_j)/2$, since the relations (B16)—(B18) tell us that

$$\tfrac{1}{2}(\mathbf{p}_1-\mathbf{p}_2)=\frac{1}{\sqrt{2}}\mathbf{p}_\rho\ , \tag{B35}$$

and the obvious corollary

$$\tfrac{1}{2}(\mathbf{p}_1-\mathbf{p}_3)=\frac{1}{\sqrt{2}}\mathbf{p}_{\rho'}\ . \tag{B36}$$

Then, for example, the factor appearing in V_{12}^{Coul} has the matrix elements

$$\delta_{S_\alpha S_\beta}\delta_{L_\alpha L_\beta}\delta_{l_{\rho_\alpha}l_{\rho_\beta}}\delta_{n_{\lambda_\alpha}n_{\lambda_\beta}}\delta_{l_{\lambda_\alpha}l_{\lambda_\beta}}\left\langle n_{\lambda_\alpha}l_{\lambda_\alpha}\left|\left[1+\frac{\frac{1}{2}p_\rho^2}{\frac{1}{2}p_\rho^2+m_1^2}\right]^{1/2+\epsilon_{\text{Coul}}}\right|n_{\lambda_\beta}l_{\lambda_\beta}\right\rangle\ , \tag{B37}$$

where

$$\left\langle n_{\lambda_\alpha}l_{\lambda_\alpha}\left|\left[1+\frac{\frac{1}{2}p_\rho^2}{\frac{1}{2}p_\rho^2+m_1^2}\right]^{1/2+\epsilon_{\text{Coul}}}\right|n_{\lambda_\beta}l_{\lambda_\beta}\right\rangle=(-i)^{-N_\alpha+N_\beta}\left\langle n_{\rho_\alpha}l_{\rho_\alpha}\left|\left[1+\frac{\frac{1}{2}\rho^2}{\frac{1}{2}\rho^2+m_1^2}\right]^{1/2+\epsilon_{\text{Coul}}}\right|n_{\rho_\beta}l_{\rho_\beta}\right\rangle_{1/\alpha}\ . \tag{B38}$$

Similar expressions hold for the other (12) momentum-dependent factor (A21); the (13) terms are calculated in much the same way except in their case there are two masses involved.

---

*Present address: Department of Theoretical Physics, University of Oxford, 1 Keble Road, Oxford OX1 3NP, United Kingdom.

[1]M. Gell-Mann, Phys. Lett. **8**, 214 (1964); G. Zweig, CERN Report No. 8182/Th.401, 1964 (unpublished); CERN Report No. 8419/Th.412, 1964 (unpublished).

[2]R. H. Dalitz, in *High Energy Physics, 1965 Les Houches Lectures,* edited by C. DeWitt and M. Jacob (Gordon and Breach, New York, 1966); O. W. Greenberg, Phys. Rev. Lett. **13**, 598 (1964); G. Morpurgo, Physics **2**, 95 (1965); O. W. Greenberg and M. Resnikoff, Phys. Rev. **163**, 1844 (1967); D. R. Digvi and O. W. Greenberg, *ibid.* **175**, 2024 (1968); R. R. Horgan, Nucl. Phys. **B71**, 514 (1974).

[3]C. Becchi and G. Morpurgo, Phys. Rev. **149**, 1284 (1966); **140**, B687 (1965); Phys. Lett. **17**, 352 (1965); R. G. Moorhouse, Phys. Rev. Lett. **16**, 771 (1966); A. N. Mitra and M. Ross, Phys. Rev. **158**, 1630 (1967); D. Faiman and A. W. Hendry, *ibid.* **173**, 1720 (1968); H. J. Lipkin, Phys. Rep. **8C**, 173 (1973); R. L. Rosner, *ibid.* **11C**, 189 (1974); R. Horgan, in *Proceedings of the Topical Conference on Baryon Resonances, Oxford, 1976,* edited by R. T. Ross and D. H. Saxon (Rutherford Laboratory, Chilton, Didcot, England, 1977), p. 435; A. Le Yaouanc *et al.*, Phys. Rev. D **11**, 1272 (1975); L. A. Copley, G. Karl, and E. Obryk, Phys. Lett. **29B**, 117 (1969); Nucl. Phys. **B13**, 303 (1969); D. Faiman and A. W. Hendry, Phys. Rev. **180**, 1572 (1969); Kohichi Ohta, Phys. Rev. Lett. **43**, 1201 (1979); R. P. Feynman, M. Kislinger, and F. Ravndal, Phys. Rev. D **3**, 2706 (1971); R. G. Moorhouse and N. H. Parsons, Nucl. Phys. **B62**, 109 (1973); see also Refs. 21, 32, and Forsyth and Cutkosky in Ref. 11.

[4]H. Lipkin and S. Meshkov, Phys. Rev. Lett. **14**, 670 (1965); D. Faiman and A. W. Hendry, Phys. Rev. **173**, 1720 (1968); **180**, 1609 (1969); E. W. Colglazier and J. L. Rosner, Nucl. Phys. **B27**, 349 (1971); W. Petersen and J. Rosner, Phys. Rev. D **6**, 820 (1972); D. Faiman and D. E. Plane, Nucl. Phys. **B50**, 379 (1972); A. J. G. Hey, P. J. Litchfield, and R. J. Cashmore, *ibid.* **B95**, 516 (1975); F. Gilman and I. Karliner, Phys. Rev. D **10**, 2194 (1974); J. Babcock and J. Rosner, Ann. Phys.

(N.Y.) **96**, 191 (1976); J. Babcock *et al.*, Nucl. Phys. **B126**, 87 (1977).

[5]O. W. Greenberg, Phys. Rev. Lett. **13**, 598 (1964).

[6]M. Y. Han and Y. Nambu, Phys. Rev. **139**, B1006 (1965); S. L. Adler, *ibid.* **177**, 2426 (1969); R. Jackiw and K. Johnson, *ibid.* **182**, 1459 (1969); S. L. Adler and W. A. Bardeen, *ibid.* **182**, 1517 (1969); M. Fritzsch, M. Gell-Mann, and H. Leutwyler, Phys. Lett. **47B**, 365 (1973); C. N. Yang and R. Mills, Phys. Rev. **96**, 191 (1954); G. 't Hooft and M. Veltman, Nucl. Phys. **B44**, 189 (1972); B. W. Lee and J. Zinn-Justin, Phys. Rev. D **5**, 3121 (1972); **5**, 3137 (1972); **5**, 3155 (1972); **7**, 1049 (1973); H. D. Politzer, Phys. Rev. Lett. **30**, 1346 (1973); D. Gross and F. Wilczek, *ibid.* **30**, 1343 (1973); S. Weinberg, Phys. Rev. D **8**, 3497 (1973); Phys. Rev. Lett. **31**, 494 (1973). For a review of QCD, see H. D. Politzer, Phys. Rep. **14C**, 129 (1974); W. Marciano and H. Pagels, *ibid.* **36C**, 137 (1979).

[7]N. Isgur, in *The New Aspects of Subnuclear Physics,* proceedings of the XVI International School of Subnuclear Physics, Erice, 1978, edited by A. Zichichi (Plenum, New York, 1980), p. 107; N. Isgur, in *Particles and Fields—1981: Testing the Standard Model,* proceedings of the Meeting of the Division of Particles and Fields of the APS, Santa Cruz, California, edited by C. A. Heusch and W. T. Kirk (AIP, New York, 1982), p. 1.

[8]A. J. G. Hey and R. Kelly, Phys. Rep. **96**, 71 (1983); O. W. Greenberg, Annu. Rev. Nucl. Part. Phys. **28**, 327 (1978); A. J. G. Hey, in *Proceedings of the European Physical Society International Conference on High Energy Physics, Geneva, 1979,* edited by A. Zichichi (CERN, Geneva, 1980); J. Rosner, in *Techniques and Concepts of High Energy Physics,* proceedings of the NATO Advanced Study Institute, St. Croix, 1980, edited by T. Ferbel (Plenum, New York, 1981); R. H. Dalitz, Nucl. Phys. **A353**, 251 (1981).

[9]For meson references, consult Ref. 16 below.

[10]N. Isgur and G. Karl, Phys. Lett. **72B**, 109 (1977); **74B**, 353 (1978); Phys. Rev. D **18**, 4187 (1978); **19**, 2653 (1979); L. A. Copley, N. Isgur, and G. Karl, *ibid.* **20**, 768 (1979); N. Isgur and G. Karl, *ibid.* **21**, 3175 (1980); K. Maltman and N. Isgur, *ibid.* **22**, 1701 (1980); K. T. Chao, N. Isgur, and G. Karl, *ibid.* **23**, 155 (1981); N. Isgur, G. Karl, and D. W. L. Sprung, *ibid.* **23**, 163 (1981); N. Isgur, G. Karl, and R. Koniuk, Phys. Rev. Lett. **41**, 1269 (1978); Phys. Rev. D **25**, 2394 (1982).

[11]A. De Rujula, H. Georgi, and S. L. Glashow, Phys. Rev. D **12**, 147 (1975); T. DeGrand, R. L. Jaffe, K. Johnson, and J. Kiskis, *ibid.* **12**, 2060 (1975); D. Gromes and I. O. Stamatescu, Nucl. Phys. **B112**, 213 (1976); T. A. DeGrand and R. L. Jaffe, Ann. Phys. (N.Y.) **100**, 425 (1976); R. H. Dalitz, in *Fundamentals of Quark Models,* proceedings of the Seventeenth Scottish Universities Summer School in Physics, St. Andrews, 1976, edited by I. M. Barbour and A. T. Davies (SUSSP, Edinburgh, Scotland, 1977); W. Celmaster, Phys. Rev. D **15**, 1391 (1977); D. Gromes, Nucl. Phys. **B130**, 18 (1977); M. Jones, R. H. Dalitz, and R. R. Horgan, *ibid.* **B129**, 45 (1977); L. J. Reinders, J. Phys. G **4**, 1241 (1978); U. Ellwanger, Nucl. Phys. **B139**, 422 (1978); M. Böhm, Z. Phys. C **3**, 321 (1980); J. M. Richard and P. Taxil, Ann. Phys. (N.Y.) **127**, 62 (1980); R. K. Bhaduri, L. E. Cohler, and Y. Nogami, Phys. Rev. Lett. **44**, 1369 (1980); Nuovo Cimento **65**, 376 (1981); D. P. Stanley and D. Robson, Phys. Rev. Lett. **45**, 235 (1980); P. J. Corvi, J. Phys. G **7**, 255 (1981); C. P. Forsyth and R. E. Cutkosky, Phys. Rev. Lett. **46**, 576 (1981); Z. Phys. C **18**, 219 (1983); R. E. Cutkosky and R. E. Hendrick, Phys. Rev. D **16**, 786 (1977); *ibid.* **16**, 793 (1977); R. Sartor and Fl. Stancu, *ibid.* **31**, 128 (1985); D. Gromes, Z. Phys. C **22**, 265 (1984); **26**, 401 (1984). See also Refs. 26, 27, and 33.

[12]A. B. Henriques, B. H. Kellet, and R. G. Moorhouse, Phys. Lett. **64B**, 85 (1976); H. Schnitzer, *ibid.* **65B**, 239 (1976); **69B**, 477 (1977); Phys. Rev. D **18**, 3483 (1978); Lai-Him Chan, Phys. Lett. **71B**, 422 (1977); L. J. Reinders, in *Baryon 1980,* proceedings of the IVth International Conference on Baryon Resonances, Toronto, 1980, edited by N. Isgur (University of Toronto Press, Toronto, 1981), p. 203; D. Gromes, Z. Phys. C **18**, 249 (1983).

[13]N. Isgur and J. Paton, Phys. Lett. **124B**, 247 (1983); Phys. Rev. D **31**, 2910 (1985). For a flux-tube model of the baryon potential, see also Refs. 33 and 34.

[14]J. Merlin and J. Paton, J. Phys. G **11**, 439 (1985).

[15]C. Hayne and N. Isgur, Phys. Rev. D **25**, 1944 (1982).

[16]S. Godfrey and N. Isgur, Phys. Rev. D **32**, 189 (1985).

[17]The use of such flavor basis functions was, to the best of our knowledge, first advocated in J. Franklin, Phys. Rev. **172**, 1807 (1968).

[18]See B. L. Moisewitch, *Variational Principles* (Wiley Interscience, New York, 1966) for a proof of this theorem.

[19]S. Godfrey (private communication).

[20]See, for example, Stephen Godfrey, Phys. Rev. D **31**, 2375 (1985).

[21]R. Koniuk and N. Isgur, Phys. Rev. Lett. **44**, 485 (1980); Phys. Rev. D **21**, 1868 (1980); R. Koniuk, in *Baryon 1980* (Ref. 12), p. 217. For other related work on baryon couplings, see Ref. 3.

[22]See De Rujula, Georgi, and Glashow in Ref. 11.

[23]See Hey, Litchfield, and Cashmore, and Faiman and Plane in Ref. 4. See also Ref. 21.

[24]J. W. Darewych, R. Koniuk, and N. Isgur, Phys. Rev. D **32**, 1765 (1985).

[25]See for example J. J. Sakurai, Ann. Phys. (N.Y.) **11**, 1 (1960); R. C. Arnold and J. J. Sakurai, Phys. Rev. **128**, 2808 (1962); R. H. Dalitz, T. C. Wong, and G. Rajasekaran, *ibid.* **153**, 1617 (1967); H. W. Wyld, *ibid.* **155**, 1649 (1967); R. K. Logan and H. W. Wyld, *ibid.* **158**, 1467 (1967); F. E. Close and R. H. Dalitz, in *Proceedings of the Workshop on Low and Intermediate Energy Kaon-Nuclon Physics, Rome, 1980,* edited by E. Ferrari and G. Violini (Reidel, Dordrecht, 1981), p. 411; D. Gromes, Z. Phys. C **18**, 249 (1983); Reinders (Ref. 12); E. A. Veit *et al.*, Phys. Lett. **137B**, 415 (1984).

[26]R. K. Bhaduri, B. K. Jennings, and J. C. Waddington, Phys. Rev. D **29**, 2051 (1984); M. V. N. Murthy, M. Dey, J. Dey, and R. K. Bhaduri, *ibid.* **30**, 152 (1984).

[27]R. E. Cutkosky, in *Proceedings of the Topical Conference in Baryon Resonances, Oxford, 1976,* edited by R. T. Ross and D. H. Saxon (Rutherford Laboratory, Chilton, Didcot, England, 1977); R. E. Cutkosky *et al.*, Nucl. Phys. **B102**, 139 (1976); see also Cutkosky and Hendrick in Ref. 11, and Hey and Kelly in Ref. 8.

[28]K. C. Bowler *et al.*, Phys. Rev. Lett. **45**, 97 (1980); P. J. Corvi, J. Phys. G **7**, 255 (1977). See also Hey and Kelly in Ref. 8.

[29]For a review of these predictions, see T. E. Barnes, in *Proceedings of the 1984 Workshop on Electron and Photon Interactions at Intermediate Energies, Bad Honnef, Germany, 1984,* edited by D. Menze, W. Pfeil, and W. J. Schwille (Lecture Notes in Physics Vol. 234) (Springer, Berlin, 1984), p. 124.

[30]See Maltman and Isgur in Ref. 10.

[31]R. Kokoski and N. Isgur, Phys. Rev. D (to be published).

[32]L. Micu, Nucl. Phys. **B10**, 521 (1961); A. Le Yaouanc, L. Oliver, O. Pene, and J. C. Raynal, Phys. Rev. D **8**, 2223 (1973); **9**, 1415 (1974); **11**, 1272 (1975); M. Chaichian and R.

Kogerler, Ann. Phys. (N.Y.) **124**, 61 (1980).

[33]I. Barbour and D. K. Ponting, Z. Phys. C **4**, 119 (1980); J. Carlson, J. B. Kogut, and V. R. Pandharipande, Phys. Rev. D **27**, 233 (1983); **28**, 2807 (1983).

[34]H. G. Dosch and V. Müller, Nucl. Phys. **B116**, 470 (1976).

[35]E. Eichten and F. L. Feinberg, Phys. Rev. D **23**, 2724 (1981); W. Buchmüller, Phys. Lett. **112B**, 479 (1982); M. A. Peskin, in *Dynamics and Spectroscopy at High Energy,* proceedings of the 11th SLAC Summer Institute on Particle Physics, edited by Patricia M. McDonough (SLAC, Stanford, CA, 1984), p. 151; D. Gromes, Z. Phys. C **22**, 265 (1984); **26**, 401 (1984). See also D. Gromes, in *The Quark Structure of Matter,* proceedings of the Yukon Advanced Study Institute, Yukon, Canada, 1984, edited by N. Isgur, G. Karl, and P. J. O'Donnell (World Scientific, Singapore, 1985), p. 1.

[36]A. J. Casher, J. Kogut, and L. Susskind, Phys. Rev. D **10**, 732 (1974). For a treatment of QCD in two dimensions, see G. 't Hooft, Nucl. Phys. **B75**, 461 (1974).

[37]H. Osborn, Phys. Rev. **176**, 1523 (1968); F. E. Close and H. Osborn, Phys. Lett. **34B**, 400 (1971); F. E. Close and L. A. Copley, Nucl. Phys. **B19**, 477 (1980); F. E. Close and R. H. Dalitz, paper presented at the *Workshop on Low and Intermediate Energy Kaon-Nucleon Physics, Rome, 1980* (Ref. 25); see also Reinders in Ref. 5.